

AD/A-001 100

ESTIMATION OF SEISMIC DETECTION
THRESHOLDS

Frode Ringdal

Texas Instruments, Incorporated

Prepared for:

Advanced Research Projects Agency
Air Force Technical Applications Center

28 May 1974

DISTRIBUTED BY:

NTIS

National Technical Information Service
U. S. DEPARTMENT OF COMMERCE



ALEX(01)-TR-74-02

ESTIMATION OF SEISMIC DETECTION THRESHOLDS

12

AD A 001 100

TECHNICAL REPORT NO. 2

VELA NETWORK EVALUATION AND AUTOMATIC PROCESSING RESEARCH

Prepared by
Frøde Ringdal

TEXAS INSTRUMENTS INCORPORATED
Equipment Group
Post Office Box 6015
Dallas, Texas 75222

Prepared for
AIR FORCE TECHNICAL APPLICATIONS CENTER
AFTAC Project No. VELA T/4705/B/ETR
Alexandria, Virginia 22314

Sponsored by
ADVANCED RESEARCH PROJECTS AGENCY
Nuclear Monitoring Research Office
ARPA Program Code No. 4F10
ARPA Order No. 2551

28 May 1974

DDC
RECEIVED
NOV 19 1974
B

Acknowledgment: This research was supported by the Advanced Research Projects Agency, Nuclear Monitoring Research Office, under Project VELA-UNIFORM, and accomplished under the technical direction of the Air Force Technical Applications Center under Contract No. F08606-74-C-0033.

Reproduced by
NATIONAL TECHNICAL
INFORMATION SERVICE
U.S. Department of Commerce
Springfield VA 22151

ii

Equipment Group

DISTRIBUTION STATEMENT A

Approved for public release
Distribution Unlimited

87

UNCLASSIFIED

SECURITY CLASSIFICATION OF THIS PAGE (When Data Entered)

REPORT DOCUMENTATION PAGE		READ INSTRUCTIONS BEFORE COMPLETING FORM
1. REPORT NUMBER	2. GOVT ACCESSION NO.	3. RECIPIENT'S CATALOG NUMBER
4. TITLE (and Subtitle) ESTIMATION OF SEISMIC DETECTION THRESHOLDS		5. TYPE OF REPORT & PERIOD COVERED Technical
		6. PERFORMING ORG. REPORT NUMBER ALEX(01)-TR-74-02 ✓
7. AUTHOR(s) Frode Ringdal		8. CONTRACT OR GRANT NUMBER(s) F08606-74-C-0033 ✓
9. PERFORMING ORGANIZATION NAME AND ADDRESS Texas Instruments Incorporated Equipment Group Dallas, Texas 75222		10. PROGRAM ELEMENT PROJECT, TASK AREA & WORK UNIT NUMBERS VELA T/4705/B/ETR
11. CONTROLLING OFFICE NAME AND ADDRESS Advanced Research Projects Agency Nuclear Monitoring Research Office Arlington, Virginia 22209		12. REPORT DATE 28 May 1974
14. MONITORING AGENCY NAME & ADDRESS (if different from Controlling Office) Air Force Technical Applications Center VELA Seismological Center Alexandria, Virginia 22314		13. NUMBER OF PAGES 88
		15. SECURITY CLASS. (of this report) UNCLASSIFIED
16. DISTRIBUTION STATEMENT (of this Report) APPROVED FOR PUBLIC RELEASE, DISTRIBUTION UNLIMITED		
17. DISTRIBUTION STATEMENT (of the abstract entered in Block 20, if different from Report)		
18. SUPPLEMENTARY NOTES ARPA Order No. 2551		
19. KEY WORDS (Continue on reverse side if necessary and identify by block number) Seismology Maximum likelihood estimation Seismic detection capability Simulation Detection thresholds Statistics		
20. ABSTRACT (Continue on reverse side if necessary and identify by block number) <p>This report deals with the general problem of estimating the incremental detection capability of a seismic station, i. e., the probability of detection as a function of event magnitude. A maximum likelihood procedure is introduced to estimate the station detection thresholds by comparison with an independent reference station or network. Approximate confidence limits for the estimated parameters are computed. The</p>		

2

UNCLASSIFIED

SECURITY CLASSIFICATION OF THIS PAGE(When Data Entered)

20. continued

results obtained by this (direct) method are compared to estimates derived from applying the exponential magnitude-frequency relationship of natural seismicity. It is found that the latter (indirect) method in general gives significantly lower 90 percent detection thresholds. This is explained theoretically as resulting from the fact that the indirect method fails to take into account the global variance of observed signal amplitudes for given seismic events. It is concluded that, if a good reference system is available, the direct method will produce estimates that are more reliable than those provided by the indirect method.

lia

UNCLASSIFIED

SECURITY CLASSIFICATION OF THIS PAGE(When Data Entered)

ACKNOWLEDGMENTS

The author would like to acknowledge D. G. Lambert and T. W. Harley for their valuable comments and suggestions during the preparation of this paper. In particular, he wishes to thank Mrs. C. B. Saunders, who typed all of the text and drafted many of the figures of this report.

ABSTRACT

This report deals with the general problem of estimating the incremental detection capability of a seismic station, i. e. , the probability of detection as a function of event magnitude. A maximum likelihood procedure is introduced to estimate the station detection thresholds by comparison with an independent reference station or network. Approximate confidence limits for the estimated parameters are computed. The results obtained by this (direct) method are compared to estimates derived from applying the exponential magnitude-frequency relationship of natural seismicity. It is found that the latter (indirect) method in general gives significantly lower 90 percent detection thresholds. This is explained theoretically as resulting from the fact that the indirect method fails to take into account the global variance of observed signal amplitudes for given seismic events. It is concluded that, if a good reference system is available, the direct method will produce estimates that are more reliable than those provided by the indirect method.

Neither the Advanced Research Projects Agency nor the Air Force Technical Applications Center will be responsible for information contained herein which has been supplied by other organizations or contractors, and this document is subject to later revision as may be necessary. The views and conclusions presented are those of the authors and should not be interpreted as necessarily representing the official policies, either expressed or implied, of the Advanced Research Projects Agency, the Air Force Technical Applications Center, or the US Government.

TABLE OF CONTENTS

SECTION	TITLE	PAGE
	ABSTRACT	iii
I.	INTRODUCTION	I-1
II.	THE GAUSSIAN MODEL FOR EVENT DETECTION PROBABILITY	II-1
	A. SINGLE STATION	II-1
	B. A NETWORK OF STATIONS	II-13
III.	MAXIMUM LIKELIHOOD ESTIMATION	III-1
	A. DIRECT ESTIMATION METHOD - GENERAL DESCRIPTION	III-1
	B. DERIVATION OF APPROXIMATE CONFIDENCE LIMITS	III-4
	C. SIMULATION	III-10
	D. INDIRECT ESTIMATION METHOD	III-16
IV.	DATA ANALYSIS	IV-1
	A. DIRECT ESTIMATION METHOD	IV-1
	B. COMPARISON OF THE DIRECT AND INDIRECT ESTIMATION METHODS	IV-10
V.	SUMMARY AND CONCLUSIONS	V-1
VI.	REFERENCES	VI-1
	APPENDIX A	A-1

LIST OF FIGURES

FIGURE	TITLE	PAGE
II-1	ILLUSTRATION OF THE GAUSSIAN HYPOTHESIS OF STATION DETECTION THRESHOLD MAGNITUDE AND STATION EVENT MAGNITUDE DISTRIBUTION	II-2
II-2	EXAMPLE SHOWING THEORETICAL NORSAR DETECTION CURVES IN TERMS OF NORSAR MAGNITUDES, LASA MAGNITUDES, AND "TRUE" MAGNITUDES	II-9
II-3	THEORETICAL DETECTION CURVES FOR SIMPLIFIED SEISMIC NETWORKS (ALL STATIONS ARE ASSUMED OF IDENTICAL CAPABILITIES AND ONE STATION DETECTION IS REQUIRED FOR NETWORK DETECTION). GAUSSIAN APPROXIMATIONS TO THE CURVES ARE ALSO SHOWN	II-14
III-1	EXAMPLE OF EVENT MAGNITUDE DISTRIBUTION AND DETECTION/NO DETECTION STATUS (100 EVENTS)	III-9
III-2	EXAMPLE OF DIRECT MAXIMUM LIKELIHOOD ESTIMATION OF A DETECTION CURVE (100 EVENTS)	III-9
III-3	MAXIMUM LIKELIHOOD ESTIMATES OF DETECTION PARAMETERS (μ, σ) BASED UPON 100 SIMULATED CASES, AND THEORETICAL 90 PERCENT CONFIDENCE ELLIPSE (100 EVENTS CASE, DIRECT ESTIMATION)	III-13
III-4	EXAMPLE OF EVENT MAGNITUDE DISTRIBUTION AND DETECTION/NO DETECTION STATUS (20 EVENTS)	III-14
III-5	EXAMPLE OF DIRECT MAXIMUM LIKELIHOOD ESTIMATION OF A DETECTION CURVE (20 EVENTS)	III-14

LIST OF FIGURES
(continued)

FIGURE	TITLE	PAGE
III-6	MAXIMUM LIKELIHOOD ESTIMATES OF DETECTION PARAMETERS (μ, σ) BASED UPON 100 SIMULATED CASES, AND THEORETICAL 90 PERCENT CONFIDENCE ELLIPSE (20 EVENTS CASE, DIRECT ESTIMATION	III-15
III-7	HISTOGRAM SHOWING THE DISTRIBUTION OF NUMBER OF EVENTS PER DAY FOR THE PDE EVENT SUMMARY DURING THE YEAR 1972. THE POISSON DISTRIBUTION WITH THE SAME MEAN IS ALSO INDICATED	III-20
III-8	INDIRECT MAXIMUM LIKELIHOOD ESTIMATES OF DETECTION PARAMETERS (μ, σ) BASED UPON 100 SIMULATED CASES	III-23
IV-1	DIRECT MAXIMUM LIKELIHOOD ESTIMATION OF THE NORSAR SP DETECTION CURVE FOR THE KURILES-KAMCHATKA REGION	IV-4
IV-2	DIRECT MAXIMUM LIKELIHOOD ESTIMATION OF THE NORSAR SP DETECTION CURVE FOR EURASIA APART FROM KURILES-KAMCHATKA	IV-5
IV-3	DIRECT MAXIMUM LIKELIHOOD ESTIMATION OF THE NORSAR LP DETECTION CURVE FOR EURASIA	IV-6
IV-4	DIRECT MAXIMUM LIKELIHOOD ESTIMATION OF A VLPE NETWORK DETECTION CURVE	IV-8
IV-5	DIRECT MAXIMUM LIKELIHOOD ESTIMATION OF THE OPERATIONAL NORSAR SP DETECTION CURVE FOR AN AFTERSHOCK SEQUENCE FROM SOUTH OF HONSHU	IV-13

LIST OF FIGURES
(continued)

FIGURE	TITLE	PAGE
IV-6	DIRECT MAXIMUM LIKELIHOOD ESTIMATION OF THE OPERATIONAL NORSAR SP DETECTION CURVE FOR AN AFTERSHOCK SEQUENCE FROM THE KURILE ISLANDS	IV-14
IV-7	NORSAR m_b VERSUS LASA m_b FOR 50 EVENTS RANDOMLY SELECTED FROM THE SOUTH HONSHU AFTERSHOCKS	IV-16
IV-8	NORSAR m_b VERSUS LASA m_b FOR 50 EVENTS RANDOMLY SELECTED FROM THE KURILE ISLANDS AFTERSHOCKS	IV-17
IV-9	DETECTION STATISTICS FOR THE INDIRECT MAXIMUM LIKELIHOOD METHOD APPLIED TO NORSAR SP OPERATIONAL PERFORMANCE FOR THE SOUTH HONSHU AFTERSHOCK SEQUENCE	IV-19
IV-10	DETECTION STATISTICS FOR THE INDIRECT MAXIMUM LIKELIHOOD METHOD APPLIED TO NORSAR SP OPERATIONAL PERFORMANCE FOR THE KURILE ISLANDS AFTERSHOCK SEQUENCE	IV-20
A-1	NORSAR VERSUS LASA BODYWAVE MAGNITUDES FOR EVENTS FROM THE KURILE ISLANDS AFTERSHOCK SEQUENCE JUNE 17-30, 1973	A-5

LIST OF TABLES

TABLE	TITLE	PAGE
IV-1	RESULTS FROM DIRECT MAXIMUM LIKELIHOOD ESTIMATION USING VARIOUS SUBSETS OF THE REFERENCE EVENT SET (VLPE NETWORK 2, GAUSSIAN MODEL)	IV-9
IV-2	NORSAR AND LASA EVENT DETECTION PERFORMANCE FOR EARTHQUAKE SWARMS FROM SOUTH HONSHU (DEC- EMBER 3-20, 1972) AND THE KURILE ISLANDS (JUNE 17-30, 1973)	IV-11
IV-3	COMPARISON BETWEEN DETECTION PARAMETER ESTIMATES OBTAINED BY THE DIRECT AND INDIRECT METHODS FOR THE NORSAR SP OPERATIONAL PERFORMANCE FOR TWO AFTERSHOCK SEQUENCES	IV-22

SECTION I INTRODUCTION

The detection capability of a seismic station or network for events from a specific region is usually referred to in terms of its incremental detection probability. This is defined as the probability of detecting an event, given the event magnitude. In particular, the 90 percent detection threshold is often quoted as a measure of performance; this is the magnitude at which the station is expected to detect 90 percent of all events.

Several methods have been devised to estimate the detection probability function of a seismic system. In general, such methods can be assigned to one of three main classes:

- Estimates based on seismic noise studies - By measuring the seismic noise level, estimating the signal-to-noise ratio required for detection and assuming a signal variance, one can reasonably well predict the actual detection performance of a system.
- Estimates based on seismicity and observed detection performance - This is a two step procedure. First the seismicity of a region is estimated by extrapolating the observed data, using the exponential magnitude-frequency relationship. Then the observed number of events is compared to the estimated seismicity in order to establish detection thresholds.
- Estimates based on comparison to a reference system - A set of events reported by an independent reference system is first selected. The percentage actually detected at each magnitude

by the station in question is then used to obtain threshold estimates.

We will in this report refer to the second and third estimation methods described above as indirect and direct estimation, respectively.

The main topic of this report is to present a new approach to the direct method of estimation, using a maximum likelihood technique. Examples of application are included, and the results are compared to those obtained by other methods.

Section II of this report establishes a model of the detection probability function which has been found useful for threshold estimation. In this model, the probability of detecting an event of a given magnitude m is assumed to be a cumulative Gaussian distribution function:

$$P(\text{Detect } m) = \Phi \left(\frac{m - \mu}{\sigma} \right) \quad (1-1)$$

where μ and σ are unknown parameters. It is shown that the parameters should be interpreted differently according to which method of estimation is being used. This has the very important implication that different methods of estimation may be expected to produce different results, so that a careful interpretation is necessary.

In Section III the likelihood function for the direct estimation method is developed, and approximate confidence limits for the estimated parameters are computed. The validity of the approximations is examined by applying a simulation model. We also include a brief description of a maximum likelihood method for the indirect estimation problem, as developed by Lacoss and Kelly (1969). We choose an approach which is slightly different from theirs in order to show that no hypothesis of Poisson distribution of natural seismicity is required to develop the likelihood function.

Section IV presents some examples showing how the direct estimation technique can be applied in practical situations. A comparison between the results obtained by the direct and indirect methods is carried out for two aftershock sequences recorded by the NORSAR and LASA arrays. It is found that the two methods yield significantly different results, but that the apparent disagreement can be adequately explained by the considerations presented in Section II.

The main results from this report are summarized in Section V.

SECTION II

THE GAUSSIAN MODEL FOR EVENT DETECTION PROBABILITY

This section addresses the general problem of establishing a model for the detection probability curve of a seismic system, i. e., the probability that the system detects an event as a function of event magnitude m .

The case of single station or seismic array detection is discussed first, and it is shown that under reasonable assumptions the detection curve will have the form of a Gaussian distribution function:

$$P(\text{Detect}/m=x) = (2\pi\sigma^2)^{-1/2} \cdot \int_{-\infty}^x e^{-\frac{(t-\mu)^2}{2\sigma^2}} dt \quad (\text{II-1})$$

This holds true whether the magnitude m is defined as the magnitude estimated by a specific station or as a "true" event magnitude measured by a hypothetical "perfect" network. However, the resulting values of the parameters μ and σ will be different in the two cases.

The detection probability curve of a seismic network is also discussed briefly. It is concluded that the Gaussian model does not apply directly to this case, but that it may still be useful as an approximation to part of the detection curve.

A. SINGLE STATION

1. Derivation of the Detection Probability

In order to determine the probability of a seismic station or array detecting an event from a specified region, we make the following assumptions (illustrated in Figure II-1):

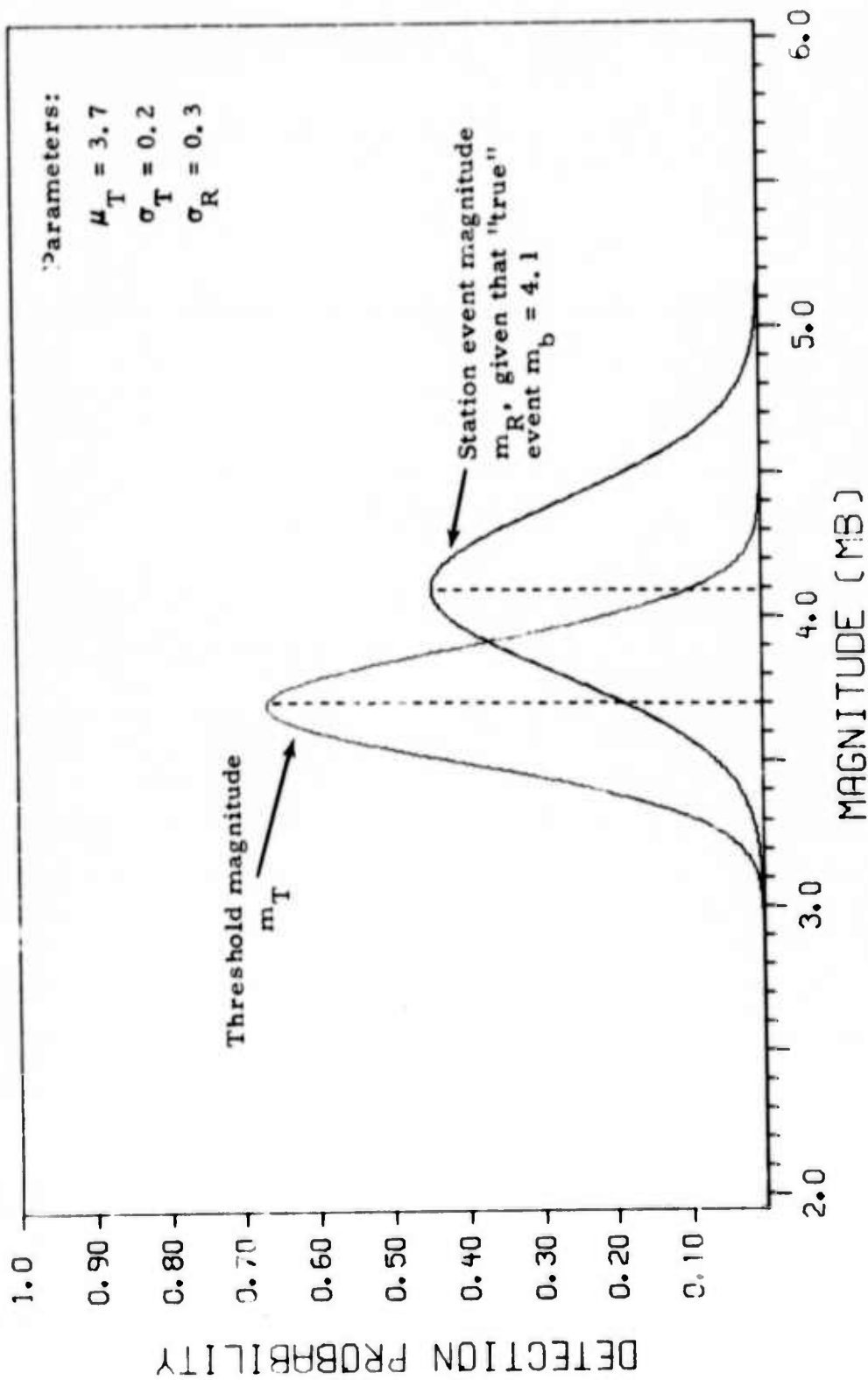


FIGURE II-1
 ILLUSTRATION OF THE GAUSSIAN HYPOTHESIS OF STATION DETECTION
 THRESHOLD MAGNITUDE AND STATION EVENT MAGNITUDE DISTRIBUTION

- Given that an event has true magnitude $m=x$, then the magnitude m_R of the corresponding signal arriving at the station is a normal variable: $m_R \sim N(x, \sigma_R^2)$.
- The event is detected at the station provided $m_R > m_T$, where m_T is a threshold magnitude determined by the seismic noise level and the characteristics of the detection algorithm. We assume that m_T is a normal variable: $m_T \sim N(\mu_T, \sigma_T^2)$.
- The random variables m_R and m_T are assumed independent.

Under these assumptions, the probability of detection, given $m=x$, is as follows:

$$\begin{aligned} P(\text{Detect}/m=x) &= P(m_R > m_T/m=x) \\ &= P(m_R - m_T > 0/m=x) \end{aligned} \quad (\text{II-2})$$

Since the conditional distribution of $(m_R - m_T)$, given $m=x$, is Gaussian, we obtain:

$$P(\text{Detect}/m=x) = \Phi \left(\frac{x - \mu_T}{\sigma} \right) \quad (\text{II-3})$$

where

$$\sigma^2 = \sigma_T^2 + \sigma_R^2 \quad (\text{II-4})$$

and Φ denotes the standard cumulative Gaussian distribution function.

The validity of this model for station detection capability rests, of course, with the validity of assuming a normal distribution for m_R and m_T .

- For the station magnitude m_R , the normality assertion means that for a given event, world wide observed magnitudes follow a

normal distribution, with a standard deviation σ_R that arises mainly from source effects and differences in radiation patterns. This has been substantiated by several studies (Lanz, 1966; Freedman 1967). Furthermore, we assume that the variance of this distribution is independent of event magnitude. To our knowledge, this has not been explicitly demonstrated by any author, although data from Bungum and Husebye (1974) comparing NORSAR and PDE magnitudes give some support to this assertion.

- For the threshold magnitude m_T , the main influencing random factor is the time variability of the noise level for the station. Evidence for a lognormal distribution of the seismic noise amplitudes for a given station as a function of time has been found by Gerlach et al., (1966) and Alsup and Becker (1973) and is supported by results from Barnard and Whitelaw (1972). Obviously, a lognormal distribution of noise amplitudes implies a normal distribution of noise "magnitudes".

Besides the above considerations, we mention briefly some additional factors that influence the distributions of m_R and m_T . Measurement errors of amplitude and period are obvious examples, another potential source is systematic errors in the distance factor. The spectral characteristics of the received signal are important for detectability purposes, and therefore influence m_T , whether an automatic detector or visual inspection is applied. In the automatic detector case, our normality assumption means that filter SNR gain (in dB) is normally distributed. Similarly, the distribution of beamforming loss influences the variance of m_T in the case of an array station.

One final important consideration is the effects of applying the Gaussian model to events within a large region. In this case, the normality assumption is only valid if the geographic seismicity distribution of the region

is such that the observed B-factors are normally distributed. This is clearly not valid in general; therefore, it is necessary to require that the model only be applied to a region for which the variation in B-factors are negligible compared to the variation of the other components in our random model.

This last requirement is not very restrictive, for example, over the epicentral distance 30-80 degrees, the bodywave distance factor varies only by $\pm 0.1 m_b$ units. This is well below the value of $\sigma_R = 0.4$ found by Veith and Clawson (1972) as a typical value of the standard deviation of magnitude measurements at single sensor stations, assuming that standard B-factor tables are used. In the case of large aperture arrays, such as LASA and NORSAR, one can expect a lower value of σ_R , due to the fact that local effects are smoothed out when the signal is averaged over a number of sensors. A value of σ_R between 0.25 and 0.30 seems reasonable in these two cases; thus the B-factor variation is still relatively insignificant.

2. Examples of Application

In the following subsection several examples are given of possible situations to which the Gaussian model could be applied. It is important to note the conditional nature of the probability expression II-3, since this is the key to a proper understanding of the various viewpoints that are presented.

To be specific, let us analyze three cases; dealing with the NORSAR P-wave detection probability in terms of "true" m_b , NORSAR m_b and LASA m_b , respectively. We will assume that:

- Given that an event has "true" magnitude $m=x$, then
 - the distribution of the NORSAR magnitude m_N is $N(x + b_N, \sigma_N^2)$
 - the distribution of the LASA magnitude m_L is $N(x + b_L, \sigma_L^2)$

- The NORSAR "threshold magnitude" m_T is $N(\mu_T, \sigma_T^2)$
- The random variables m_N , m_L , and m_T are independent.

a. NORSAR Detection Curve in Terms of "True" Magnitude m

Given that $m=x$, then m_N is $N(x+b_N, \sigma_N^2)$, so that

$$\begin{aligned}
 P(\text{Detect}/m=x) &= P(m_N > m_T / m=x) \\
 &= \Phi \left(\frac{(x - \mu_T) + b_N}{\sigma_1} \right) \quad (\text{II-5})
 \end{aligned}$$

where

$$\sigma_1^2 = \sigma_T^2 + \sigma_N^2 \quad (\text{II-6})$$

b. NORSAR Detection Curve in Terms of NORSAR Magnitude m_N .

In this case, the problem is to determine the probability of detection, given that a signal arrives at NORSAR corresponding to a magnitude $m_N = x$. (Thus it is implicitly assumed that the signal has an m_N value even if it is not detected.)

Given that $m_N = x$, it is clear that detection occurs provided $x > m_T$, so that

$$P(\text{Detect}/m_N=x) = \Phi \left(\frac{x - \mu_T}{\sigma_T} \right) \quad (\text{II-7})$$

It is evident that an indirect procedure is required in order to estimate NORSAR detectability in terms of m_N . One such procedure would be to analyze the distribution of the seismic noise level, and thereby estimate

μ_T and σ_T . Another procedure is to assume that the number of earthquakes $N(x)$ exceeding a given NORSAR magnitude x may be expressed by

$$\log N(x) = a - bx \quad (\text{natural logarithm}). \quad (\text{II-8})$$

and use this expression in conjunction with the observed number of events to determine detection thresholds, (Lacoss and Kelly, 1969; Bungum and Husebye, 1974).

Note that the formula (II-8) is more commonly expressed in terms of base 10 logarithms. If this is done, a and b become $a' = a/\log 10$ and $b' = b/\log 10$, respectively.

c. NORSAR Detection Curve in Terms of LASA Magnitude m_L .

Given that $m_L = x$, it is not a straightforward task to find the distribution of m_N . It will be shown in Appendix A that the conditional distribution of m_N is Gaussian, and that

$$E(m_N/m_L = x) = x - b\sigma_L^2 + (b_N - b_L) \quad (\text{II-9})$$

$$\text{Var}(m_N/m_L = x) = \sigma_L^2 + \sigma_N^2 \quad (\text{II-10})$$

if it is assumed that only earthquakes (as opposed to explosions) are considered, and that the seismicity observed at LASA may be expressed by (II-8). The correction factor $-b\sigma_L^2$ in (II-9) arises from the skew distribution of earthquake magnitudes, and is typically around 0.1 m_b units.

From the above considerations, it is easy to show that the NORSAR detection probability in terms of LASA m_b values becomes

$$P(\text{Detect}/m_L = x) = \Phi \left(\frac{x - \mu_T - b\sigma_L^2 + (b_N - b_L)}{\sigma_2} \right) \quad (\text{II-11})$$

where

$$\sigma_2^2 = \sigma_T^2 + \sigma_N^2 + \sigma_L^2 \quad (\text{II-12})$$

The NORSAR detection curve in terms of LASA magnitudes can easily be estimated directly, by selecting reference events reported by LASA and verifying whether or not a NORSAR detection occurred. (Ringdal and Whitelaw, 1973a, 1973b.)

d. Discussion

When considering the three cases discussed above, it is evident that we would desire to estimate the NORSAR detection capability in terms of a "true" magnitude as discussed under a.

A comparison of the detection curves obtained by the three methods discussed here is presented in Figure II-2 for a typical situation. It is assumed that both LASA and NORSAR are unbiased, that $\mu_T = 3.70$, $\sigma_T = 0.15$, and that $\sigma_N = \sigma_L = 0.25$. A value of $b = 2.0$ has been used (this corresponds to a slope of 0.9 in the base 10 seismicity curve).

It is seen that the 50 percent detection threshold has a slight positive bias for the curve based on LASA m_b . The 90 percent threshold in terms of the NORSAR m_b curve is significantly lower than the corresponding threshold based on LASA m_b values (by about 0.4 m_b units in this case), while the "true" 90 percent threshold is about midway between these two values.

Although we will give a more detailed discussion of how to estimate detection curves in Sections III and IV of this report, it seems appropriate to give an example of the importance of the above considerations.

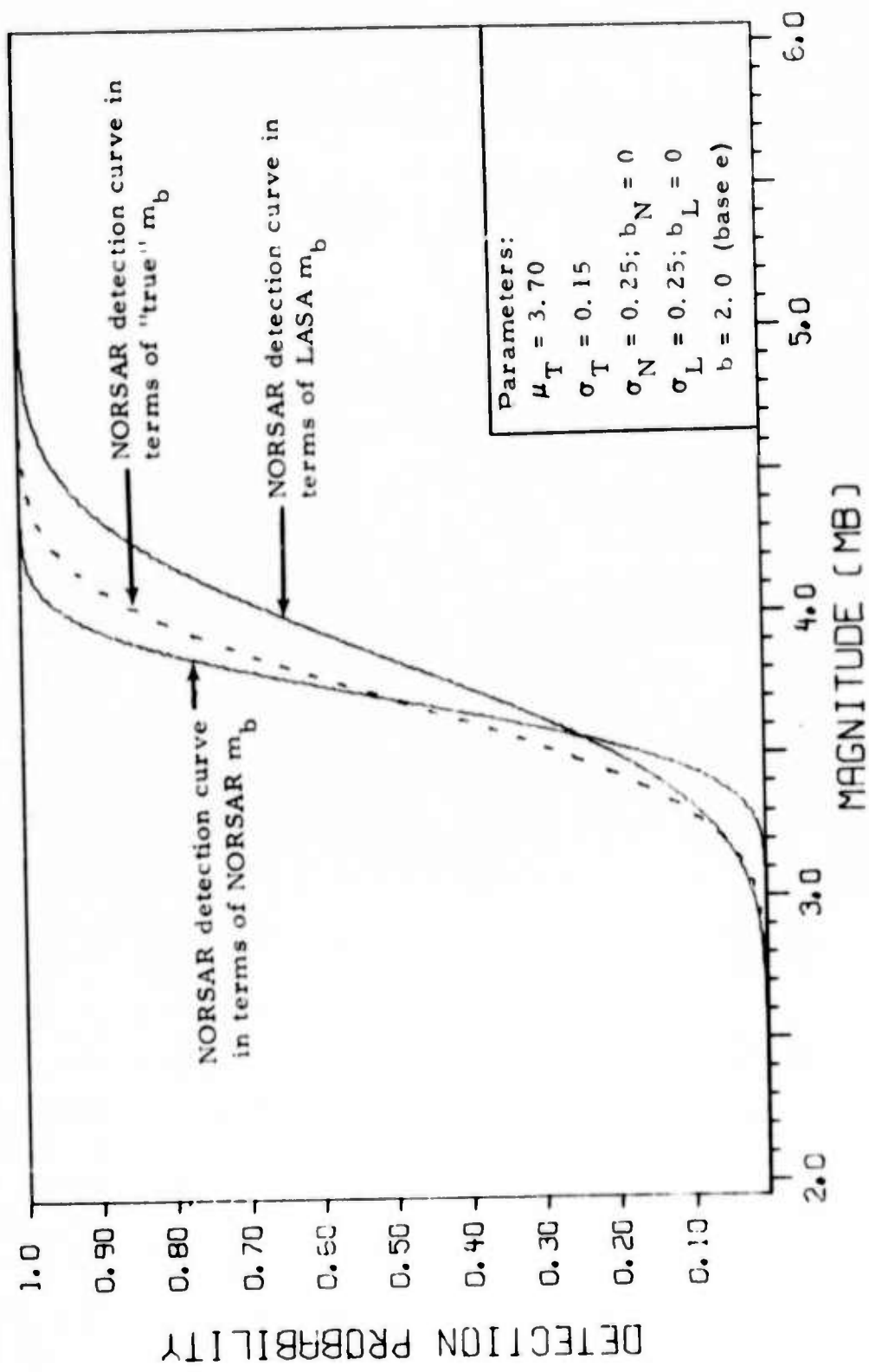


FIGURE II-2
 EXAMPLE SHOWING THEORETICAL NORSAR DETECTION CURVES
 IN TERMS OF NORSAR MAGNITUDES, LASA MAGNITUDES, AND "TRUE" MAGNITUDES

Ringdal and Whitelaw (1973b) estimate the "optimum" 90 percent incremental detection threshold for the NORSAR SP array to be slightly below $m_b = 4.3$ for the Kuriles-Kamchatka region (essentially in terms of LASA magnitudes). Yet Bungum and Husebye (1974) report that the operational NORSAR 90 percent incremental detection threshold for the same region is about $m_b = 4.0$ in terms of NORSAR magnitudes. NORSAR and LASA can be considered mutually unbiased for this region.

This apparent contradiction stems from the fact that two different detection curves are estimated in the two cases, (method b and c respectively). By the preceding considerations, we can relate both estimates to the "true" detection curve, since it is reasonable to assume that the situation illustrated in Figure II-2 applies.

In this way, we find that Bungum and Husebye's estimate corresponds to a "true" 90 percent detection threshold of $m_b = 4.1 - 4.2$, while Ringdal and Whitelaw's estimate corresponds to a "true" $m_b = 4.0 - 4.1$. Thus the apparent contradiction is removed, and the proper conclusion is that the NORSAR array has an operational capability for the Kuriles-Kamchatka region which is very close to the optimum capability that can be obtained using the beamforming/filtering detection algorithm.

3. Applications to Surface Wave Detectability

The Gaussian model described previously may also be applied to the detection probability of long period surface waves. An added consideration in this case is how to compare estimates in terms of M_s to estimates in terms of m_b . This has previously been discussed in papers by Harley and Heiting (1972) and Lacoss (1971); we will in the following briefly summarize the relevant considerations. Our assumptions are:

- Given an event of true bodywave magnitude $m=x$, then the true surface wave magnitude M is given by

$$M = f(x) + r \quad (II-13)$$

where f is a deterministic function and r is sampled from a normal distribution of zero mean and variance σ_r^2 .

- The NORSAR surface wave detection threshold magnitude M_T is normally distributed; $M_T \sim N(\mu_{MT}, \sigma_{MT}^2)$.
- Given that the true surface wave magnitude $M = y$, then the NORSAR surface wave magnitude M_N is $N(y + b_{MN}, \sigma_{MN}^2)$
- M_T and M_N are independent.
 - a. NORSAR LP Detection Curve in Terms of True Surface Wave Magnitude.

Given that $M = y$, it is found in a way similar to Example 2a that the detection probability becomes:

$$P(\text{Detect}/M=y) = \Phi \left(\frac{y - \mu_{MT} + b_{MN}}{\sigma_3} \right) \quad (II-14)$$

where

$$\sigma_3^2 = \sigma_{MN}^2 + \sigma_{MT}^2 \quad (II-15)$$

- b. NORSAR LP Detection Curve in Terms of True Bodywave Magnitude.

Given that $m=x$, it follows that M is $N(f(x), \sigma_r^2)$. It is then found that the conditional distribution of M_N is Gaussian, and that

$$E(M_N/m=x) = f(x) + b_{MN} \quad (II-16)$$

$$\text{Var}(M_N/m=x) = \sigma_{MN}^2 + \sigma_r^2 \quad (\text{II-17})$$

This implies that the NORSAR LP detection probability in terms of true body-wave magnitude m becomes:

$$P(\text{Detect}/m=x) = \Phi \left(\frac{f(x) - \mu_{MT} + b_{MN}}{\sigma_4} \right) \quad (\text{II-18})$$

where

$$\sigma_4^2 = \sigma_{MN}^2 + \sigma_{MT}^2 + \sigma_r^2 \quad (\text{II-19})$$

By comparing expression (II-18) to (II-14) it is seen that it is not correct to transfer between the two detection curves simply by substituting $y = f(x)$; one must also take the inherent scatter in the $M_s - m_b$ relationship into account.

In its simplest form the relationship between M_s and m_b is approximated by a linear function f , such as the Gutenberg-Richter (1956) relation:

$$M_s = 1.59 m_b - 3.97 \quad (\text{II-20})$$

In this linear case, the detection curve as a function of m_b becomes Gaussian. However, if f is assumed to be a non-linear function (Evernden et. al., (1971) and Tsai (1972)), this no longer holds true. In order to obtain a Gaussian curve, in this case, it is necessary to plot detectability as a function of $f(m_b)$. This of course requires that f is known a priori.

Similar considerations as given above apply to detection curves in terms of magnitude estimates that are not necessarily "true" (such as LASA magnitudes). We will not elaborate this point any further here.

B. A NETWORK OF STATIONS

It is not a straightforward task to apply the Gaussian model to seismic detection probability using a world-wide network. Clearly the detection probability is a function of the network detection algorithm; the most common algorithm is to declare an event if at least M individual stations (out of a total of N) show corresponding detections.

Under the assumptions presented earlier, let us assume that the probability of detection for station number i , given true event magnitude $m=x$, is

$$P_i(\text{Detect}/m=x) = \Phi\left(\frac{x - \mu_i}{\sigma_i}\right) \quad i = 1, 2, \dots, N \quad (\text{II-21})$$

If we set the network detection requirement to $M=1$, and assume that different stations detect the event independently, we obtain the following network detection probability.

$$P(\text{Network Detection}/m=x) = 1 - \prod_{i=1}^N \left(1 - \Phi\left(\frac{x - \mu_i}{\sigma_i}\right)\right) \quad (\text{II-22})$$

Similar expressions can readily be obtained for alternative values of M , using binomial expansion.

Clearly, the resulting detection curve is not a cumulative Gaussian distribution. An interesting question is how well it can be approximated by a Gaussian curve, and some insight into this is provided in Figure II-3. This figure shows the detection curve for a network of N stations ($N = 1, 2, 10, 100$) according to (II-22), assuming that all $\mu_i = 4.5$, $\sigma_i = 0.4$ $i = 1, 2, \dots, N$. The dashed curves are Gaussian distribution functions with the same 50 percent and 90 percent detection levels as the theoretical curves. It is seen that the Gaussian distributions give quite good approximations over limited magnitude ranges, but do not seem to fit the entire curve.

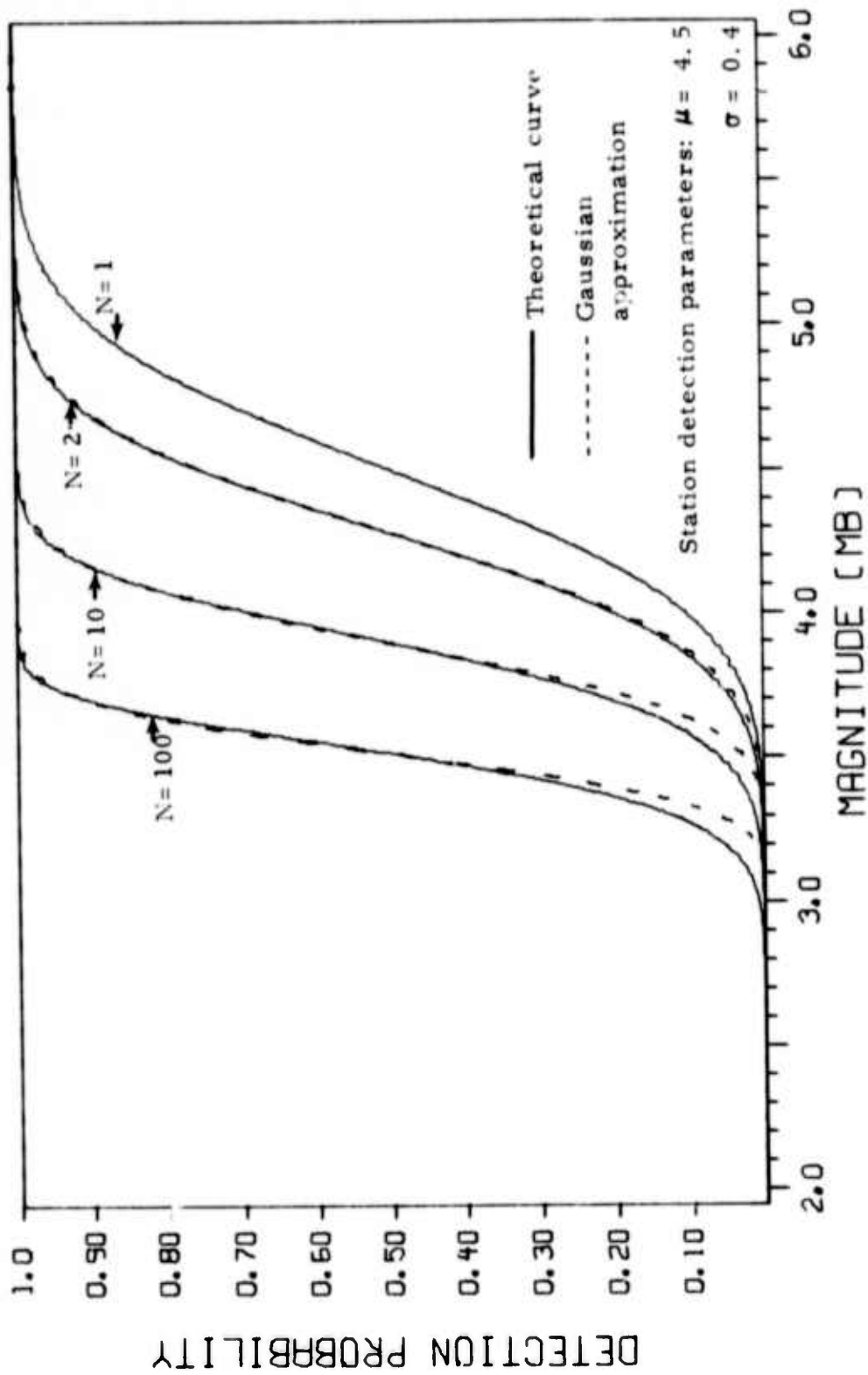


FIGURE II-3

THEORETICAL DETECTION CURVES FOR SIMPLIFIED SEISMIC NETWORKS
 (ALL STATIONS ARE ASSUMED OF IDENTICAL CAPABILITIES AND ONE
 STATION DETECTION IS REQUIRED FOR NETWORK DETECTION).
 GAUSSIAN APPROXIMATIONS TO THE CURVES ARE ALSO SHOWN

Part of the reason that the fit is not good at low magnitudes is the lack of symmetry around the 50 percent level for the theoretical curves. Actually, the case of $M=1$ gives the least symmetric detection curve; so that the Gaussian approximations will be at least as good if multi-station detection is required. The best approximation may be expected for $M = N/2$, when the theoretical curve becomes symmetric around the 50 percent level.

In practical situations, the network detection probability function is further complicated by variable detection capability of individual stations and distance factor variations. Furthermore, occasional outages of one or more stations in the network may cause loss of detections. It is clearly difficult to give general statements as to the applicability of the Gaussian model to practical network situations. However, for a reasonably stable, homogeneous network, it might be anticipated that the Gaussian model can be used as an approximation to the detection curve over limited magnitude ranges. An example of this will be studied in some detail in Section IV.

Finally, it might be observed that the network situation presents additional problems if it is desired to find the network detection probabilities in terms of the network's own magnitudes. (Similarly to Example 2b in this subsection.) This is because network magnitudes are usually computed by averaging the magnitudes of the detecting stations. Thus the network magnitudes will be biased high for events of low (true) magnitude, that are not detected by all stations. Better methods of network magnitude determination (Herrin and Tucker, 1972) would be required to overcome this problem.

SECTION III
MAXIMUM LIKELIHOOD ESTIMATION

This section presents a detailed description of the maximum likelihood method for direct detection threshold estimation. Asymptotic confidence limits are computed for the estimated parameters, and the validity of using these as approximations in practical cases is investigated by performing computer simulation. A brief description of the indirect estimation technique developed by Lacoss and Kelly (1969) is also included.

A. DIRECT ESTIMATION METHOD - GENERAL DESCRIPTION

The purpose of the estimation process described below is to estimate the "detection curve" for a seismic station or network; i. e., the probability of detection as a function of event magnitude.

The basic assumption is that the detection curve belongs to some general class of functions, and can be completely characterized by the values of a set of parameters. In particular, we will deal with the Gaussian model which was described in Section II. We recall that, in this model, the detection curve is of the general form:

$$P(m) = (2\pi\sigma^2)^{-1/2} \int_{-\infty}^m e^{-\frac{(t-\mu)^2}{2\sigma^2}} dt \quad (\text{III-1})$$

Thus, in the Gaussian case, the station detection potential is characterized by the actual values of the parameters μ and σ . The problem therefore is to estimate these two parameters.

The general procedure in estimating the parameters of the detection curve for a seismic station is as follows:

- Obtain a reference set of randomly selected events of various magnitudes (as reported by the reference source).
- For each event in the reference set, make a decision as to whether or not the station has detected this event.
- Establish the likelihood function for the observed pattern of decisions; detection versus no detection, using the general form of the detection curve.
- Find the set of parameter values of the detection curve that maximizes the likelihood function.

To establish a formal model, we will assume that the reference data base consists of n seismic events of magnitudes m_1, \dots, m_n , respectively. These magnitude values are as reported by the reference source, and must therefore be considered as statistical estimates of the true event magnitudes (see Section II). To simplify the notation, we will assume (with no loss of generality) that all the m_i values are different. (Note that m is a continuous variable.) We thus arrive at a statistical test situation, where n independent tests are carried out; for each test the probability of success (i. e., detection) is specified by equation (III-1), for the proper value of m .

Let $x_i = 1$ if the station detects the i^{th} event, $i = 1, 2, \dots, n$; $x_i = 0$ otherwise. The probability of a particular combination x_1, \dots, x_n occurring is

$$\Lambda(x_1, \dots, x_n) = \prod_{i=1}^n P(m_i)^{x_i} \cdot (1 - P(m_i))^{1 - x_i} \quad (\text{III-2})$$

For a given outcome of this experiment, $x_1 = a_1, \dots, x_n = a_n$, the maximum

likelihood estimates of μ and σ are obtained by maximizing the log likelihood function

$$\text{Log } L(\mu, \sigma) = \sum_{i=1}^n \left[a_i \cdot \text{Log } F(m_i) + (1 - a_i) \cdot \text{Log } (1 - P(m_i)) \right] \quad (\text{III-3})$$

We will denote by $\hat{\mu}$ and $\hat{\sigma}$ the pair of parameter values that maximizes (III-3).

For information about the general properties of maximum likelihood estimators, we refer to Cramer (1945). Before discussing further the mathematical aspects of the estimation method, we find it appropriate to comment briefly on some of our assumptions.

The most important assertion in the above estimation method (apart from the validity of the general form of the detection curve) is the randomness criterion in the selection of reference events. The essential point here is to select events independently of the station for which we want to estimate the detection curve. In this way, the events in the reference set, for any given magnitude, will represent a randomly chosen subset of the total number of events occurring. Thus the percent detected will be an unbiased estimate of the percentage that the station would detect of the whole event population for each magnitude.

It is clear that the procedure described here will estimate the detection curve of a seismic station in terms of magnitudes from an independent station or network. Thus the uncertainties in these magnitude estimates affect the resulting detection curve as described in Section II.

Further, it should be noted that the actual decision; detection versus no detection can be made in several ways, such as

- Check to see if the reference events have been reported in the routine seismic bulletin from the station in question (thus estimating "Operational detection threshold").

- Inspect visually the station waveforms for each reference event to verify detection or no detection (thus estimating the "event verification threshold" which might be expected to be superior to the operational threshold).
- Apply new detection algorithms to the station waveform for each reference event, thus estimating the performance of these algorithms.
- For a seismic network, determine the detection threshold as a function of the number of individual station detections required for network detection.

It is important to remember that the Gaussian model (or other models) are to be considered only as approximations to the true station detection curve. The estimation method described here is in a sense mainly a curve-fitting technique, and will work best in the magnitude range where the largest number of events are available. Inference about detection probabilities obtained by extrapolating the curve to magnitudes where data are scarce should therefore be avoided. In many cases it might be advisable to select only a specific magnitude interval of interest, and fit the Gaussian curve to the observed data in this interval. Examples of this will be given later.

B. DERIVATION OF APPROXIMATE CONFIDENCE LIMITS

1. Asymptotic Properties of the Estimators

One of the most prominent features of maximum likelihood estimators is that they often possess very desirable asymptotic properties. Under reasonably general conditions, the following may be proved (Cramer, 1945, pp 500-504).

- The solution of the likelihood equation converges in probability to the true parameter value as the number of observations increases.
- The maximum likelihood estimator is asymptotically efficient. (Informally, an efficient estimator is one that has lower variance than any other unbiased estimator).
- The maximum likelihood estimator is asymptotically normally distributed.

In order to verify that these properties apply to our particular case, we find it convenient to regard the selection of reference events as a random experiment. Thus we assume that the probability density function for selecting a reference event of magnitude m is of some fixed form, $s(m)$, and that individual selections are independent.

In this way we can view our direct estimation procedure as consisting of observing the outcomes (m, x) of n independent experiments, each with the likelihood function:

$$\Lambda_1(m, x; \mu, \sigma) = s(m) \cdot P(m)^x \cdot (1-P(m))^{1-x} \quad (\text{III-4})$$

The original likelihood function (III-2) is then equivalent to a product of n functions of the form (III-4); in the sense that the factors originating from $s(m)$ do not depend upon μ and σ , and therefore will not influence the maximum likelihood estimates.

As $n \rightarrow \infty$, we can now apply the two-dimensional form of the limiting theorem in Cramer (1945), in order to show that the asymptotic properties described above apply to our case.

2. Computation of Asymptotic Confidence Limits

Our next step is to find approximate values of the variances of $\hat{\mu}$ and $\hat{\sigma}$ and their covariance. In view of the preceding considerations, it is reasonable to compute the corresponding quantities for an unbiased, efficient estimator of μ and σ (usually known as the Cramer-Rao bounds), and use these values as approximations. Following Cramer (1945, pp 490-495) we obtain:

$$\left[\text{Var} (\hat{\mu}) \right]^{-1} \simeq (1 - \rho^2(\hat{\mu}, \hat{\sigma})) \cdot E \left(\frac{\partial \text{Log } L}{\partial \mu} \right)^2 \quad (\text{III-5})$$

$$\left[\text{Var} (\hat{\sigma}) \right]^{-1} \simeq (1 - \rho^2(\hat{\mu}, \hat{\sigma})) \cdot E \left(\frac{\partial \text{Log } L}{\partial \sigma} \right)^2 \quad (\text{III-6})$$

$$\text{Cov} (\hat{\mu}, \hat{\sigma}) = \rho(\hat{\mu}, \hat{\sigma}) \cdot \left[\text{Var} (\hat{\mu}) \cdot \text{Var} (\hat{\sigma}) \right]^{1/2} \quad (\text{III-7})$$

In the above formulae, E denotes the statistical expectation, with the sample space consisting of all possible outcomes x_1, \dots, x_n of detections/no detections, each combination of x_i 's having a probability of occurrence defined by equation (III-2).

The correlation coefficient $\rho(\hat{\mu}, \hat{\sigma})$ used in the above expressions can be approximated by

$$\rho(\hat{\mu}, \hat{\sigma}) \simeq -E \left(\frac{\partial \text{Log } L}{\partial \mu} \cdot \frac{\partial \text{Log } L}{\partial \sigma} \right) \cdot \left[E \left(\frac{\partial \text{Log } L}{\partial \mu} \right)^2 \cdot E \left(\frac{\partial \text{Log } L}{\partial \sigma} \right)^2 \right]^{-1/2} \quad (\text{III-8})$$

Because of the simple form of the likelihood functions (III-2) and (III-3), it is relatively easy to obtain analytic expressions of the quantities

defined in equations (III-5) through (III-8). By carrying out the necessary computations, and in particular observing the independence of the n test situations, we find (setting $P(m_i) = P_i$):

$$E\left(\frac{\partial \text{Log } L}{\partial \mu}\right)^2 = \sum_{i=1}^n P_i^{-1} \cdot (1 - P_i)^{-1} \cdot \left(\frac{\partial P_i}{\partial \mu}\right)^2 \quad (\text{III-9})$$

$$E\left(\frac{\partial \text{Log } L}{\partial \mu} \cdot \frac{\partial \text{Log } L}{\partial \sigma}\right) = \sum_{i=1}^n P_i^{-1} \cdot (1 - P_i)^{-1} \cdot \left(\frac{\partial P_i}{\partial \mu}\right) \left(\frac{\partial P_i}{\partial \sigma}\right) \quad (\text{III-10})$$

$$E\left(\frac{\partial \text{Log } L}{\partial \sigma}\right)^2 = \sum_{i=1}^n P_i^{-1} \cdot (1 - P_i)^{-1} \cdot \left(\frac{\partial P_i}{\partial \sigma}\right)^2 \quad (\text{III-11})$$

Note that expressions (III-9 through III-11) are not restricted to the Gaussian model (III-1), and that extension to classes of detection curves with more than two parameters obviously is possible.

In the Gaussian situation, the function P is given by (III-1), and we obtain after evaluating the partial derivatives:

$$E\left(\frac{\partial \text{Log } L}{\partial \mu}\right)^2 = \sum_{i=1}^n Z_i \quad (\text{III-12})$$

$$E\left(\frac{\partial \text{Log } L}{\partial \mu} \cdot \frac{\partial \text{Log } L}{\partial \sigma}\right) = \sum_{i=1}^n \left(\frac{m_i - \mu}{\sigma}\right) \cdot Z_i \quad (\text{III-13})$$

$$E\left(\frac{\partial \text{Log } L}{\partial \sigma}\right)^2 = \sum_{i=1}^n \left(\frac{m_i - \mu}{\sigma}\right)^2 \cdot Z_i \quad (\text{III-14})$$

where:

$$Z_i = \exp(-(m_i - \mu)^2 / \sigma^2) \cdot \left[2\pi\sigma^2 P(m_i) \cdot (1 - P(m_i)) \right]^{-1} \quad (\text{III-15})$$

Once the variances of $\hat{\mu}$ and $\hat{\sigma}$ and their covariance are known, it becomes easy to find the uncertainty involved in estimation e. g., of the 90 percent incremental detection threshold. In fact, according to the Gaussian model (III-1), the 90 percent limit μ_{90} is given by

$$\mu_{90} = \mu + f \cdot \sigma \quad (\text{III-16})$$

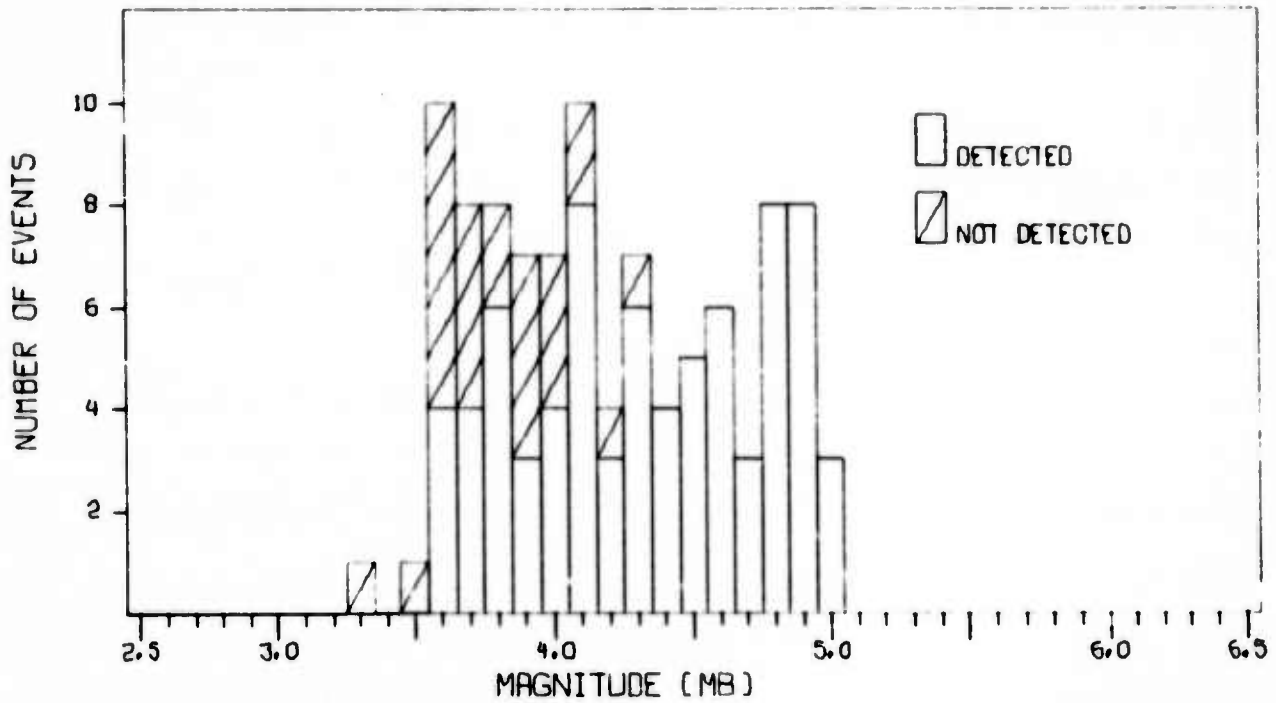
where $f = 1.28$ is the 90th percentile of the standard normal distribution. Thus we obtain an estimate $\hat{\mu}_{90}$ and its variance as follows:

$$\hat{\mu}_{90} = \hat{\mu} + f \cdot \hat{\sigma} \quad (\text{III-17})$$

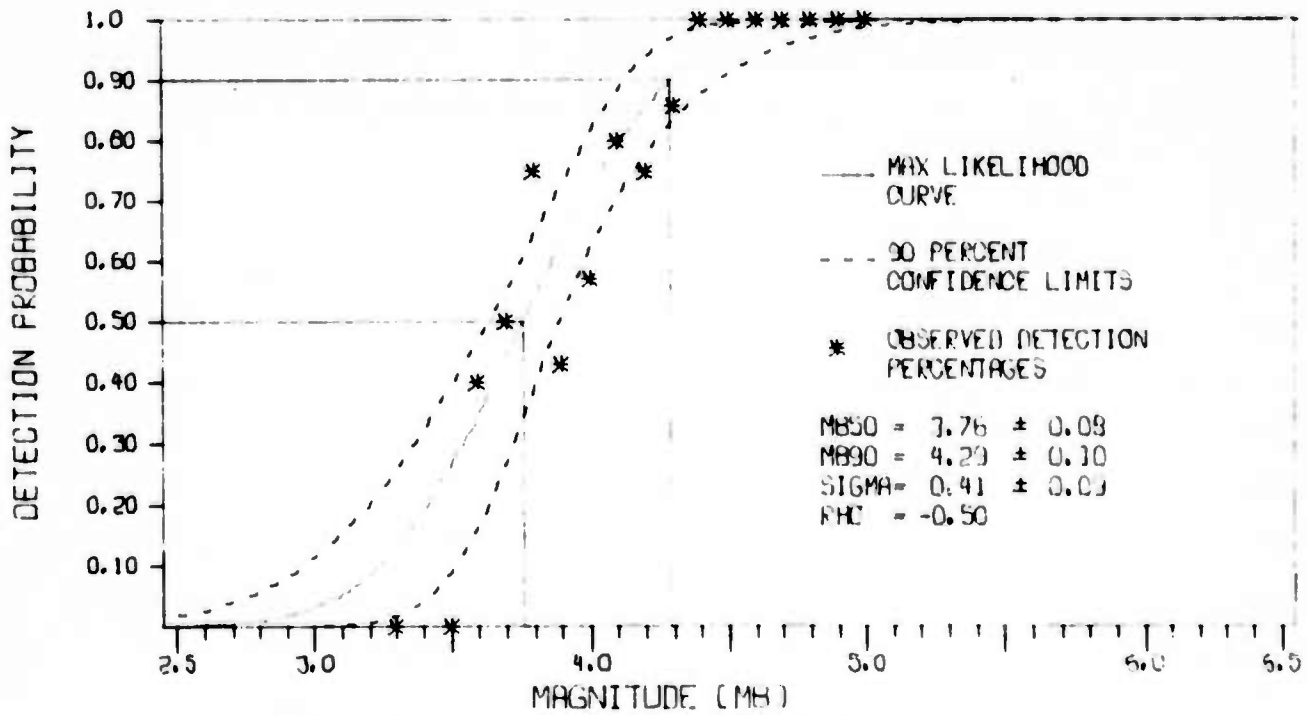
$$\text{Var}(\hat{\mu}_{90}) = \text{Var}(\hat{\mu}) + f^2 \cdot \text{Var}(\hat{\sigma}) + 2f \cdot \text{Cov}(\hat{\mu}, \hat{\sigma}) \quad (\text{III-18})$$

By assuming that $\hat{\mu}_{90}$ is approximately normally distributed, we can then use (III-17) and (III-18) to obtain confidence limits on μ_{90} .

It is in this way possible to construct "confidence curves" for the detectability curve (III-1) as shown in an example in Figures III-1 and III-2. Figure III-1 gives a hypothetical combination of events and detection status. The corresponding maximum likelihood detection curve and its 90 percent confidence limits are shown in Figure III-2. In this particular case, most events in the reference set have magnitudes greater than the apparent value of the 50% detectability limit μ . Thus, as can be expected, the confidence in the 90 percent detection estimate is greater than e. g., the confidence in the 10 percent estimate.



MB DISTRIBUTION OF PROCESSED EVENTS
 FIGURE III-1
 EXAMPLE OF EVENT MAGNITUDE DISTRIBUTION AND
 DETECTION/NO DETECTION STATUS (100 EVENTS)



MAXIMUM LIKELIHOOD DETECTABILITY CURVE
 FIGURE III-2
 EXAMPLE OF DIRECT MAXIMUM LIKELIHOOD ESTIMATION OF
 A DETECTION CURVE (100 EVENTS)

It is important to interpret these confidence curves properly. First of all, it should be pointed out that the confidence limits are derived without reference to how "well" the experimental data actually fit the Gaussian model (III-1). The term confidence in this case just means that if the detection probabilities are according to the model (III-1), then we can expect a maximum likelihood estimated based on, say, 100 events to reflect the true parameter value with the given level of confidence. However, if, for some reason, the Gaussian model (III-1) does not appropriately describe the situation, our maximum likelihood estimate as well as its confidence limits will of course be meaningless.

Secondly, the confidence limits represent a smoothing over all data points. Thus there is no reason to expect 90 percent of all the observed percentages (marked as asterisks) to lie within the 90 percent confidence limits. This becomes more evident if we decrease the size of the magnitude bins such that only one event corresponds to each magnitude. In that case all "observed" percentages will be either 0 or 100; thus all corresponding points will lie outside the 90 percent confidence limits.

C. SIMULATION

The properties of our maximum likelihood estimators derived previously in this section are only asymptotically valid. This means that although the given approximations can be expected to work well for large reference event samples, nothing is said about their validity when the number of events is limited. It is clearly important to obtain some information about how well the given expressions approximate the real distribution of the estimators in practical situations, and a convenient way to do this is to establish a simulation model. The simulation procedure is as follows:

- Assume that the detection curve is known; e. g., that the Gaussian model (III-1) is valid and that $\mu = \mu_0$, $\sigma = \sigma_0$.

- Assume further that the reference event set is specified; i. e., that the magnitude distribution m_1, \dots, m_n is known.

Under these assumptions, we are able to proceed as follows:

- Simulate the outcomes of 100 test situations, where each situation consists of the following two steps:
 - Create a pattern of decisions; detection/no detection for the reference events, using the predefined detection probabilities in a random model.
 - Find maximum likelihood estimates $\hat{\mu}$ and $\hat{\sigma}$ based upon the outcome.
- Compute the theoretical approximate 90 percent confidence ellipse for the maximum likelihood estimators; based upon the equations (III-5) through (III-8), with $\mu = \mu_0$, $\sigma = \sigma_0$.
- Compare the observed (simulated) outcomes with the theoretical confidence ellipse to determine how well the approximations work in practice.

The theoretical 90 percent confidence ellipse corresponding to two binormally distributed estimators X and Y with correlation ρ and mean and variance (m_x, σ_x^2) and (m_y, σ_y^2) respectively, is (Cramer, 1945):

$$\left(\frac{x - m_x}{\sigma_x}\right)^2 - \frac{2\rho(x - m_x)(y - m_y)}{\sigma_x \cdot \sigma_y} + \left(\frac{y - m_y}{\sigma_y}\right)^2 = a^2(1 - \rho^2) \quad (\text{III-19})$$

where a is given by

$$1 - \exp\left(-\frac{a^2}{2}\right) = 0.90 \quad (\text{III-20})$$

In our case, we can apply these equations by substituting the values given by (III-5) through (III-8) and approximating the distribution of $\hat{\mu}$ and $\hat{\sigma}$ by a joint normal distribution.

Figure III-3 presents the results from one such simulation experiment. The reference event set contained $n=100$ events, of a magnitude distribution identical to that shown in Figure III-1. Parameter values of $\mu_0 = 3.76$ and $\sigma_0 = 0.41$ were used as "true" parameters of the detection curve (III-1). The resulting 100 pairs of estimates $(\hat{\mu}, \hat{\sigma})$ are plotted in Figure III-3 together with the 90 percent confidence ellipse based upon the theoretical considerations presented earlier.

It is seen that the ellipse reflects well the simulated distribution of the estimators in this case. Thus we can conclude that the "confidence curves" of Figure III-2 covering this particular case provide reasonably accurate indications of the uncertainties in the estimated parameter values.

A second simulation case is presented in Figures III-4 through III-6. Again, a reference event set is given, this time with $n=20$ events, of a magnitude distribution as shown in Figure III-4. A hypothetical combination of detection/no detection decisions gave estimates of the detection curve as shown in Figure III-5. By simulating 100 cases with $\mu_0 = 4.10$, $\sigma_0 = 0.39$, we obtained the results presented in Figure III-6. The 90 percent confidence ellipse is seen to contain 85 of the observed values; thus reflecting reasonably well the uncertainties of the estimators. However, the distribution of points is clearly not symmetric, and for eight test cases (marked as arrows) a very large estimate of σ (greater than 1.0) was found. This indicates a lack of stability in the estimation process which we attribute to the low number of events ($n=20$) in the reference data base.

In conclusion, it is clear that no general statement can be made as to the minimum number of events n that is required for our approximations

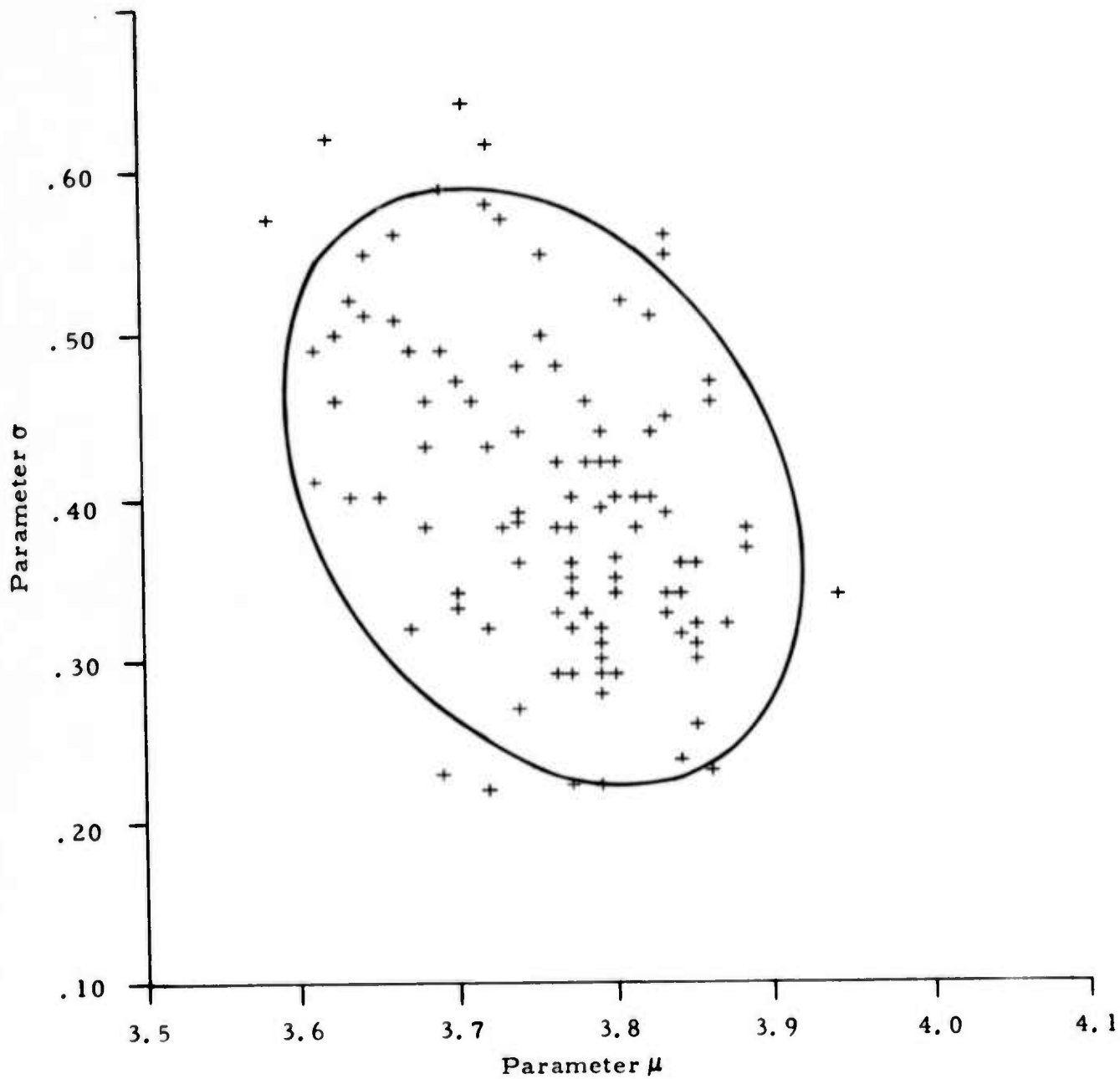
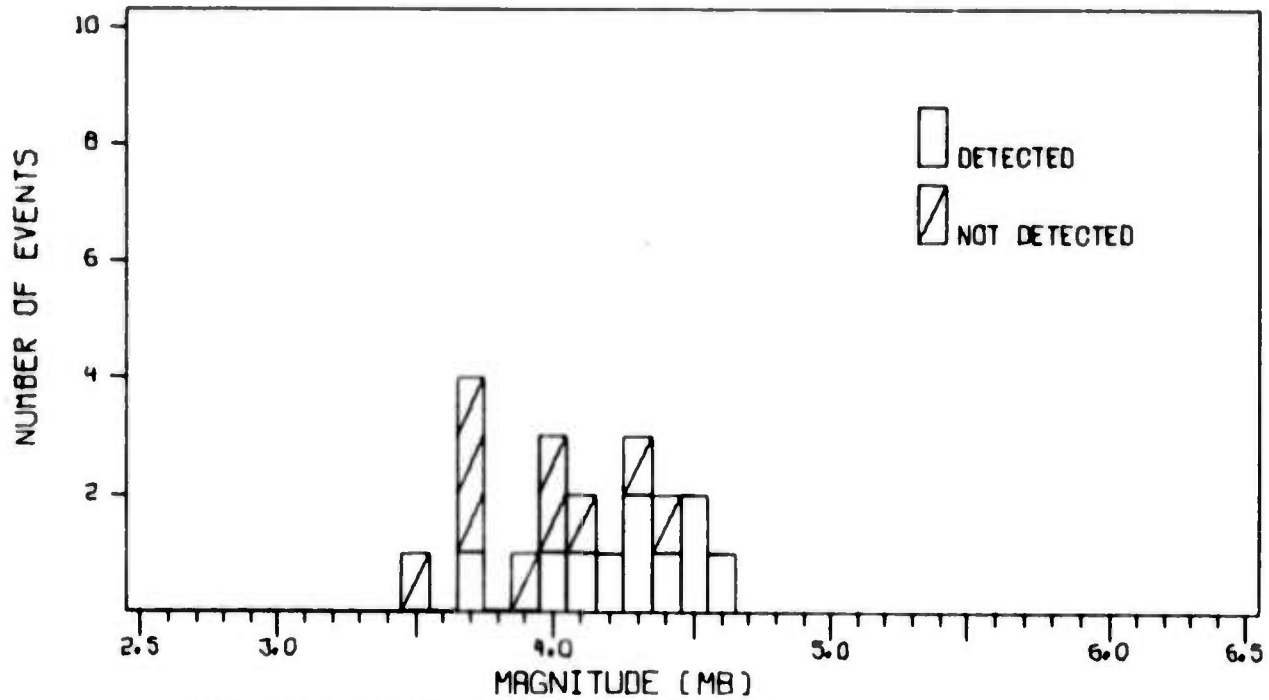


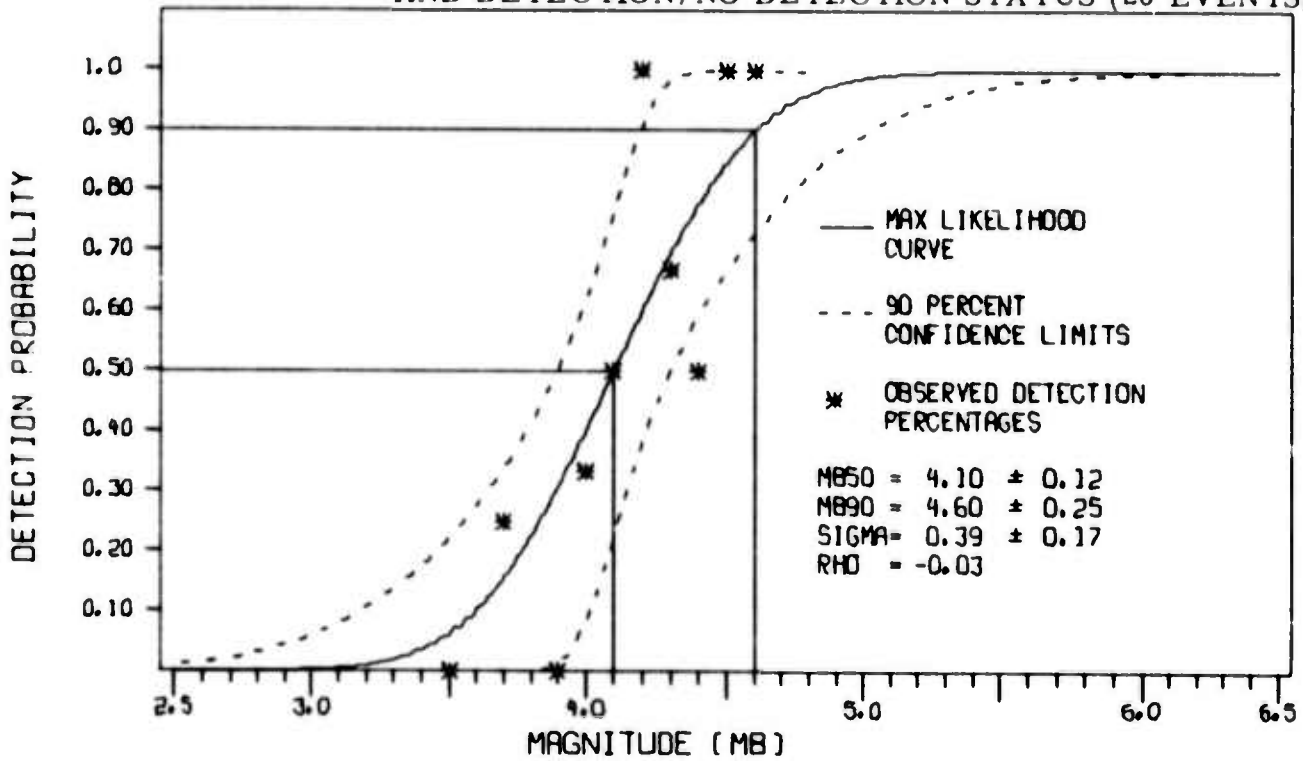
FIGURE III-3

MAXIMUM LIKELIHOOD ESTIMATES OF DETECTION PARAMETERS (μ, σ)
 BASED UPON 100 SIMULATED CASES, AND THEORETICAL
 90 PERCENT CONFIDENCE ELLIPSE
 (100 EVENTS CASE, DIRECT ESTIMATION)



MB DISTRIBUTION OF PROCESSED EVENTS

FIGURE III-4 EXAMPLE OF EVENT MAGNITUDE DISTRIBUTION AND DETECTION/NO DETECTION STATUS (20 EVENTS)



MAXIMUM LIKELIHOOD DETECTABILITY CURVE

FIGURE III-5
EXAMPLE OF DIRECT MAXIMUM LIKELIHOOD ESTIMATION OF A DETECTION CURVE (20 EVENTS)

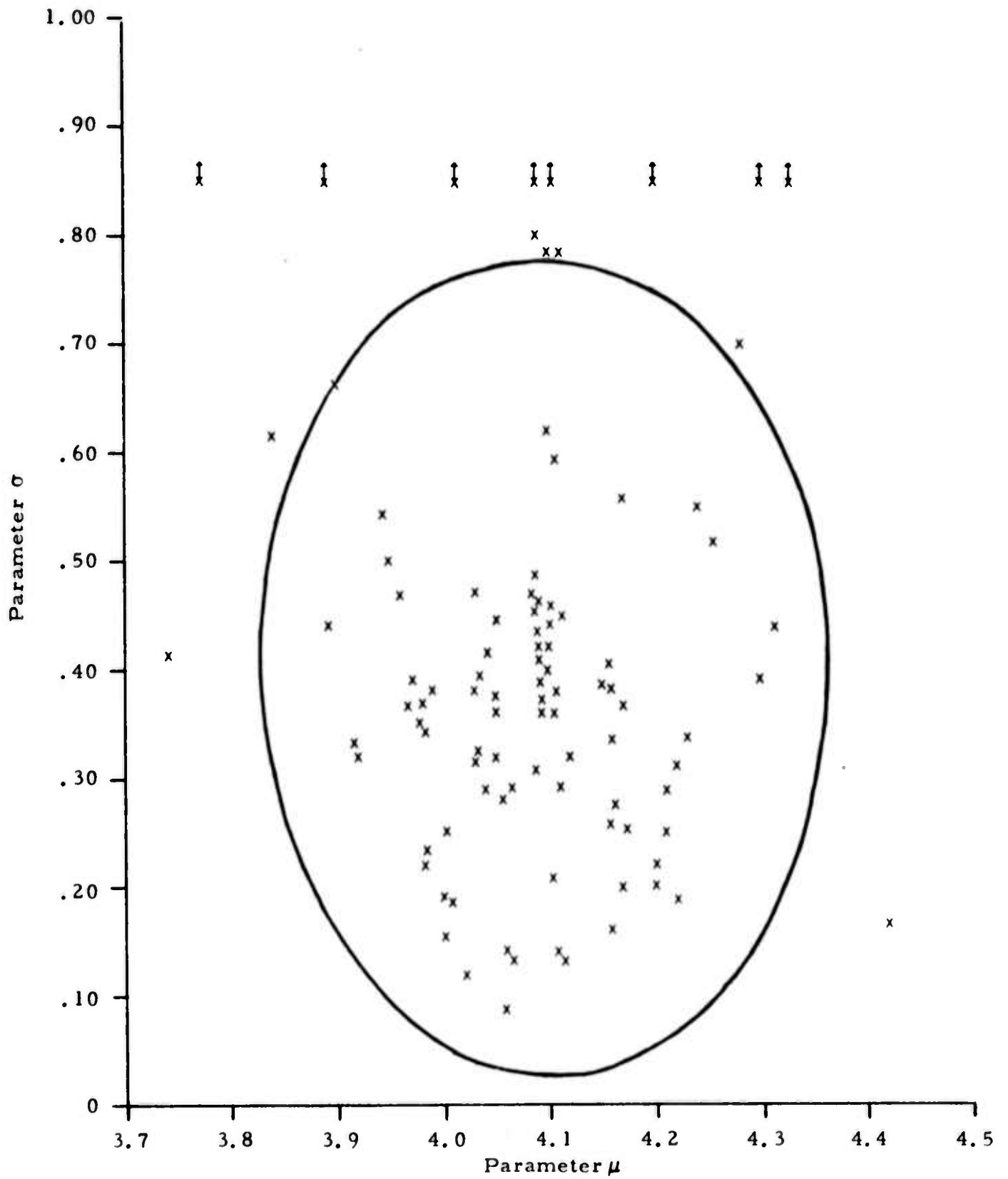


FIGURE III-6

MAXIMUM LIKELIHOOD ESTIMATES OF DETECTION PARAMETERS
 (μ, σ) BASED UPON 100 SIMULATED CASES, AND THEORETICAL
 90 PERCENT CONFIDENCE ELLIPSE (20 EVENTS CASE,
 DIRECT ESTIMATION)

to be reasonable. This is because the performance of the approximations depend on the event magnitude distribution relative to the detection curve as well as on the number n . However, it may be postulated that, given a situation with at least 100 reference events, our approximations may be used with confidence, provided that the magnitude range and the distribution of detection/no detection decisions are reasonable. For smaller event populations, the approximate confidence limits must be used only with great caution, and with the understanding that the estimation process may occasionally lead to results with a very large error margin.

D. INDIRECT ESTIMATION METHOD

Indirect estimation of detection thresholds is, in our terminology, a two-step process:

- The first step is to estimate the seismicity of a certain region over a certain time period, by observing the number of events detected by a seismic system as a function of magnitude.
- The second step is to use the estimated seismicity curve together with the observed data to estimate detection thresholds.

In practice, the seismicity is estimated by fitting the well known frequency magnitude distribution (III-21) to the data:

$$N(m) = e^{a-bm} \quad (\text{III-21})$$

where $N(m)$ is the number of events of magnitude exceeding m , and a and b are parameters that characterize the seismicity. (The corresponding base 10 parameters are $a' = a/\log 10$ and $b' = b/\log 10$ (natural logarithms) respectively.)

The actual curve fitting can be done by a least squares technique (as applied by Bungum and Husebye, 1974) or by a maximum likelihood procedure. We will prefer the second approach in the following; more specifically, we will apply a method developed by Lacoss and Kelly (1969) for joint determination of seismicity and detection parameters.

1. The Likelihood Function

Our assumptions are as follows:

- The number of detected earthquakes, K , from a specific region and their magnitudes m_1, \dots, m_k (listed in non-decreasing order) have been observed over a certain time interval by a seismic station or network.
- The seismicity corresponding to the above region and time period is given by (III-21).
- For given values of a and b , the probability $p(m)dm$ that an earthquake occurs with magnitude between m and $m+dm$ is obtained by differentiating (III-21):

$$p(m) dm = b \cdot e^{a-bm} \cdot dm \quad (\text{III-22})$$

and the occurrence of earthquakes in non-overlapping magnitude intervals are statistically independent.

The likelihood function can now be derived by assuming that a and b are given, and that the detection curve $P(m)$ is known. We choose the following informal approach, which can be extended to a formalized proof if desired:

Suppose that the magnitude axis is partitioned into small intervals of length dm . The probability of detection an event in the interval $(m, m+dm)$ is

$$F(m)dm = P(m) \cdot p(m)dm \quad (\text{III-23})$$

The probability of detecting precisely K events in the magnitude ranges $(m_i, m_i + dm_i)$ $i = 1, 2, \dots, K$, respectively, is given by:

$$L(K, m_1, \dots, m_K / a, b, P) dm_1, \dots, dm_K = \prod_{i=1}^K F(m_i) dm_i \cdot \prod_{\substack{\text{all other} \\ \text{intervals}}} (1 - F(m_j) dm_j) \quad (\text{III-24})$$

The second part of the right-hand side of (III-24) is an infinite product, and we can clearly replace it by a similar product representing all intervals on the m axis without changing its limiting value. We thus obtain:

$$\begin{aligned} \lim_{\text{all } j} \prod (1 - F(m_j) dm_j) &= \lim \exp \left(- \sum_{\text{all } j} F(m_j) dm_j \right) \\ &= \exp \left(- \int_{-\infty}^{\infty} F(m) dm \right) \end{aligned} \quad (\text{III-25})$$

where we have used the approximation $e^x \simeq 1 + x$ for small values of x . The integral in (III-25) is seen to be the total expected number of detected events N , given a , b , and P .

$$N = \int_{-\infty}^{\infty} b \cdot e^{a-bm} \cdot P(m) dm \quad (\text{III-26})$$

It is, of course, assumed that this integral converges.

The expression (III-24) for the likelihood function thus becomes:

$$L(K, m_1, \dots, m_K / a, b, P) = e^{-N} \cdot \prod_{i=1}^K b \cdot e^{a - b m_i} \cdot P(m_i) \quad (\text{III-27})$$

$$m_1 < m_2 < \dots < m_K$$

which is identical to the expression found by Lacoss and Kelly (1969), using the Poisson distribution.

We would like to point out that our derivation of the likelihood function does not assume that the observed number of earthquakes follows a Poisson distribution. This is very important, since it has repeatedly been observed that the occurrence of earthquakes cannot be adequately represented as a Poisson process. Figure III-7 shows as an example the actual distribution of the daily number of events reported by PDE during the year 1972, and compares it to the Poisson distribution with the same mean. The two distributions clearly do not match.

However, it is interesting to notice that when integrating equation (III-27) in order to obtain the marginal distribution of the number of reported events K , given a , b , and P , we find as a result the Poisson distribution, with parameter N . This is not a contradiction, it only means that if (hypothetically) our experiment could be repeated a number of times with fixed seismicity parameters a and b ; and with a constant detection probability function P , then the total number of observed events K would follow a Poisson distribution.

In practice, of course, the seismicity parameters are highly variable as a function of time (in particular the parameter a); this explains why natural seismicity does not follow the Poisson law.

It follows from the preceding considerations (by appropriate choice of the function P) that the number of earthquakes in any given magnitude range follows a Poisson distribution in the hypothetical case of constant seismicity.

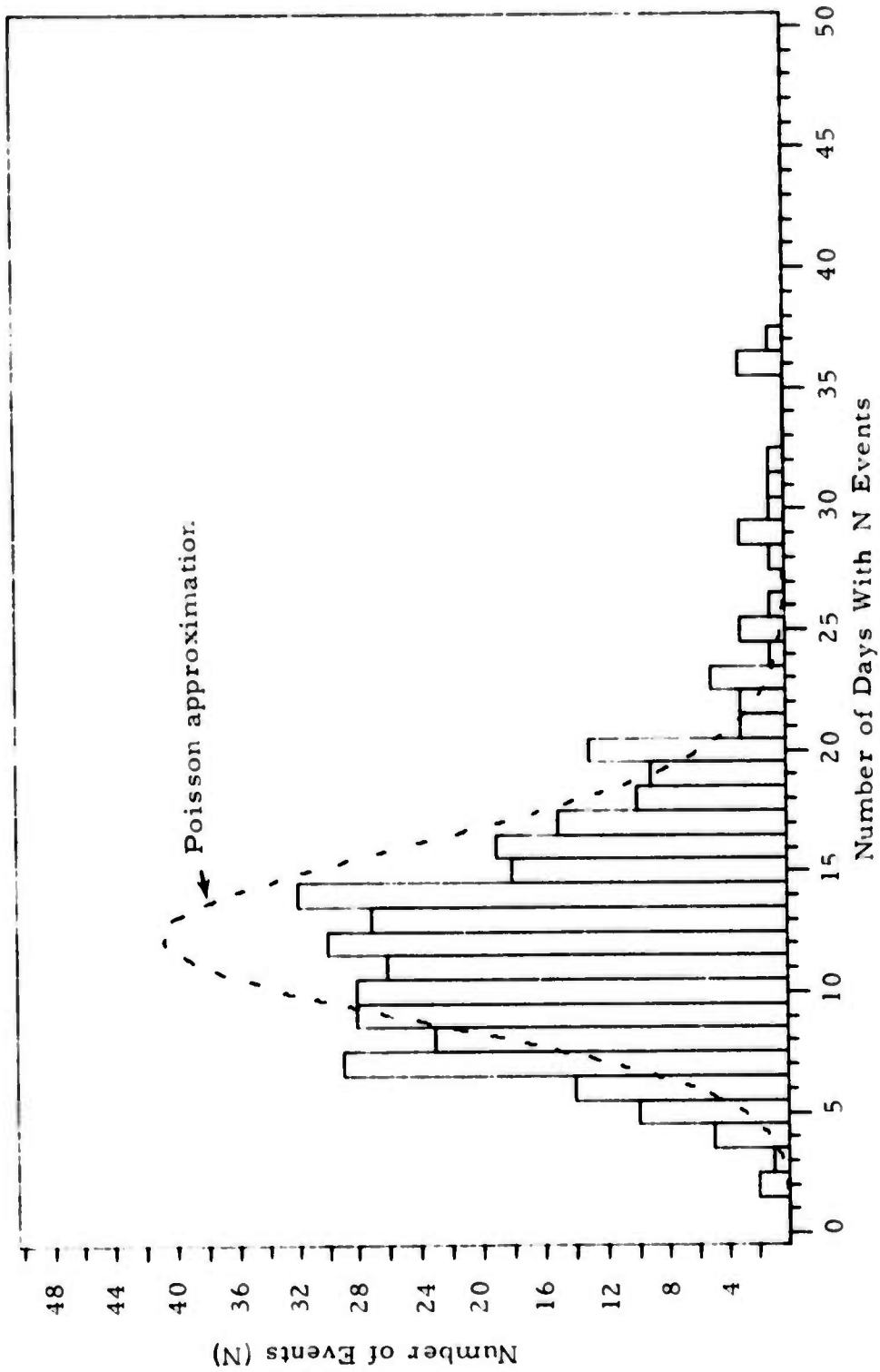


FIGURE III-7
 HISTOGRAM SHOWING THE DISTRIBUTION OF NUMBER OF EVENTS PER DAY
 FOR THE PDE EVENT SUMMARY DURING THE YEAR 1972. THE POISSON
 DISTRIBUTION WITH THE SAME MEAN IS ALSO INDICATED

2. Derivation of Estimators

We will from now on assume that the detection curve is Gaussian, i. e., that $P(m)$ is given by (III-1). This implies that the expected number of events N , is:

$$N = e^{a - b\mu + b^2\sigma^2/2} \quad (\text{III-28})$$

Following Lacoss and Kelly (1969), we obtain the maximum likelihood estimates \hat{a} and \hat{b} of a and b respectively as follows (expressed as functions of μ and σ):

$$1/\hat{b} = \frac{1}{2} (\bar{m} - \mu) \left[1 + \sqrt{1 + \frac{4\sigma^2}{(\bar{m} - \mu)^2}} \right] \quad (\text{III-29})$$

$$\hat{a} = \hat{b} \cdot \mu + \log K - \frac{\hat{b}^2 \sigma^2}{2} \quad (\text{III-30})$$

where \bar{m} is the average of the observed magnitudes. Substituting these values back into the likelihood function (III-27) then yields a function of μ and σ that can be maximized by a computer procedure. The values of μ and σ that maximize this function are the desired maximum likelihood estimates of the parameters of the detection curve.

3. A Simulation Case

In order to obtain some information about the fluctuations in the parameter estimates obtained by the indirect maximum likelihood method, we carried out a simulation experiment as follows:

Suppose that an experiment has resulted in estimate values of a , b , μ and σ . Keeping these values fixed, we can simulate the outcome of a number of similar experiments (e. g., 100), using the Poisson distribution

as a random model to obtain the number of detected events in each magnitude bin. (This is acceptable since the Poisson assumption is valid when the system parameters are fixed.) Subsequently we can estimate the parameter values based on the outcomes of the experiments, and see how they fluctuate relative to the original, "true" values.

Results from a simulation experiment are presented (for the parameters μ and σ) in Figure III-8. The original parameters were $\mu = 3.91$, $\sigma = 0.12$, $a' = 6.00$ (base 10), $b' = 1.00$ (base 10). This corresponds to an expected number of detections $N = 133$. A total of 100 cases were simulated. The results indicate the following:

- 90 percent of the estimates of μ are between 3.85 and 4.00.
- 90 percent of the estimates of σ are between 0.08 and 0.17.
- 90 percent of the estimates of b' are between 0.83 and 1.25 (not shown on the figure).

It is also observed that the distribution of points appears to be reasonably symmetric, and that no significant bias can be seen. As stated by Lacoss and Kelly (1969), the estimators possess the desirable asymptotic properties described previously for the direct estimation case; thus we know that the performance of the estimates will improve as N becomes large. It is thus concluded that the method can be applied with good confidence if several hundred events are available. However, we stress again the importance of verifying the statistical assumptions before applying the method, since outliers in the event distribution can very easily distort the resulting estimates.

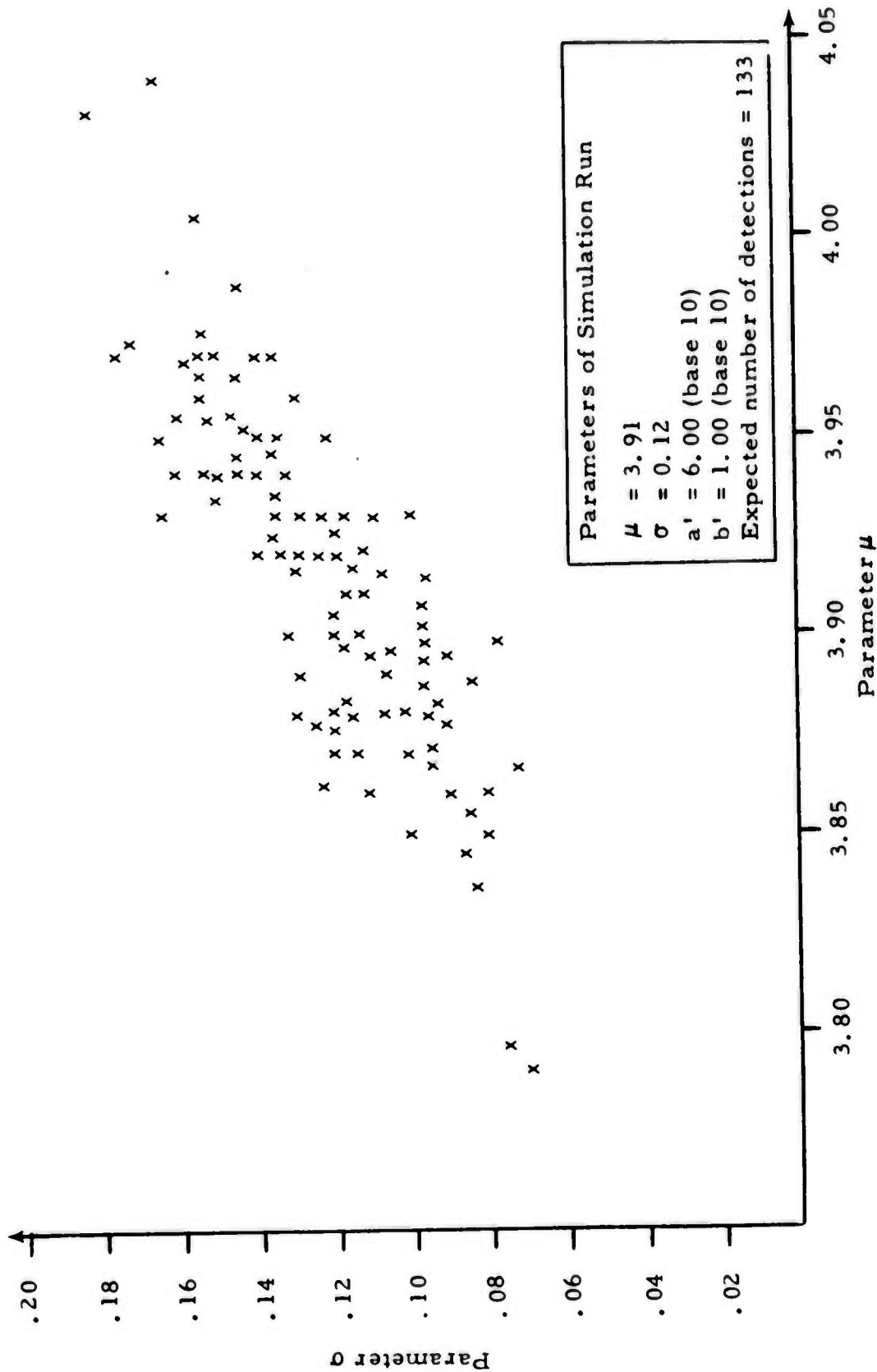


FIGURE III-8
 INDIRECT MAXIMUM LIKELIHOOD ESTIMATES OF DETECTION PARAMETERS
 (μ, σ) BASED UPON 100 SIMULATED CASES

SECTION IV DATA ANALYSIS

This section presents some examples of detection threshold estimation, with emphasis on the direct maximum likelihood method. In addition, a comparison is carried out between the direct and indirect methods of estimation, based upon data from two earthquake aftershock sequences recorded by the NORSAR and LASA arrays.

A. DIRECT ESTIMATION METHOD

In this subsection we give several examples of application of the direct estimation method to seismic stations or networks. These examples are all taken from evaluation reports published recently by Texas Instruments Incorporated. The general estimation procedure has been as follows:

- Obtain a reference event set (typically up to 500 events) from one or more of the following sources:
 - The PDE bulletin (Preliminary Determination of Epicenters from the World-Wide Seismic Network).
 - The LASA weekly event summary issued by the Seismic Data Analysis Center.
 - The NORSAR weekly event summary compiled at Kjeller, Norway.
 - The bulletin from the International Seismic Month, ISM, (February 20 - March 19, 1972) compiled at Lincoln Laboratories.

- For each event, compute the expected arrival time at the station to be evaluated, and display the waveforms for this station for a time interval covering the signal arrival.
- Make a decision as to whether or not the station has a detectable signal corresponding to this event. Usually this decision is made by the analyst, based upon visual inspection of the filtered and beamformed signal traces.
- For selected regions, compile the number of events detected and not detected by magnitude, and apply the direct maximum likelihood estimation method to determine the station detection curves for those regions.

When applying the estimation method, it must first be asserted that the conditions for validity are fulfilled. In particular, the following points should be observed:

- Independence between reference source and station to be evaluated.
- Validity of the Gaussian model. In particular the selected seismic region should be sufficiently limited in size so that B-factor variation can be ignored. Also the limitations of the Gaussian model for network detection should be remembered.
- Consistent reference magnitude estimates. This is essential to obtain unbiased estimates. While single station magnitude variance can be mathematically compensated for (Appendix A), a problem like the PDE magnitude bias for small events (Herrin and Tucker, 1972), is essentially untractable, and therefore represents a serious drawback in applying the method.

- False alarm problems. The possibility clearly exists that a "reference event" is really a false alarm. Likewise, it might happen that the analyst verifies an event by mistaking a noise burst for a signal. Caution is required to minimize bias caused by this effect.

1. NORSAR SP Detection Threshold

The detection capability of the short period NORSAR array was evaluated by Ringdal and Whitelaw (1973b). Figures IV-1 and IV-2 show the results for the two subregions; the Kuriles-Kamchatka arc and the remainder of the Eurasian continent, respectively.

Of special interest is Figure IV-2, which shows very few non-detections and hence gives an estimate of very low confidence of the 50 percent detection threshold. In fact, it might be questionable whether the Gaussian model can reasonably represent the detection curve in this case, since B-factors vary significantly over the 15° - 60° epicentral distance range for this region. Therefore statements based on extrapolation of the Gaussian curve below the magnitude range of the observed data should be avoided in this case.

2. NORSAR LP Detection Threshold

The detection capability of the NORSAR LP array has been evaluated by Laun, Shen and Swindell, (1973). The detection curve for their total earthquake ensemble as a function of bodywave magnitude is presented in Figure IV-3. It is seen that the Gaussian curve fits quite well in spite of the large epicentral distance variation involved, (20-70 degrees).

As in the case of NORSAR SP estimation, it was necessary to eliminate events that had been reported with NORSAR as the primary source. This is because SP detection and LP detection at NORSAR are not independent; clearly both probabilities fluctuate with the NORSAR microseismic noise level.

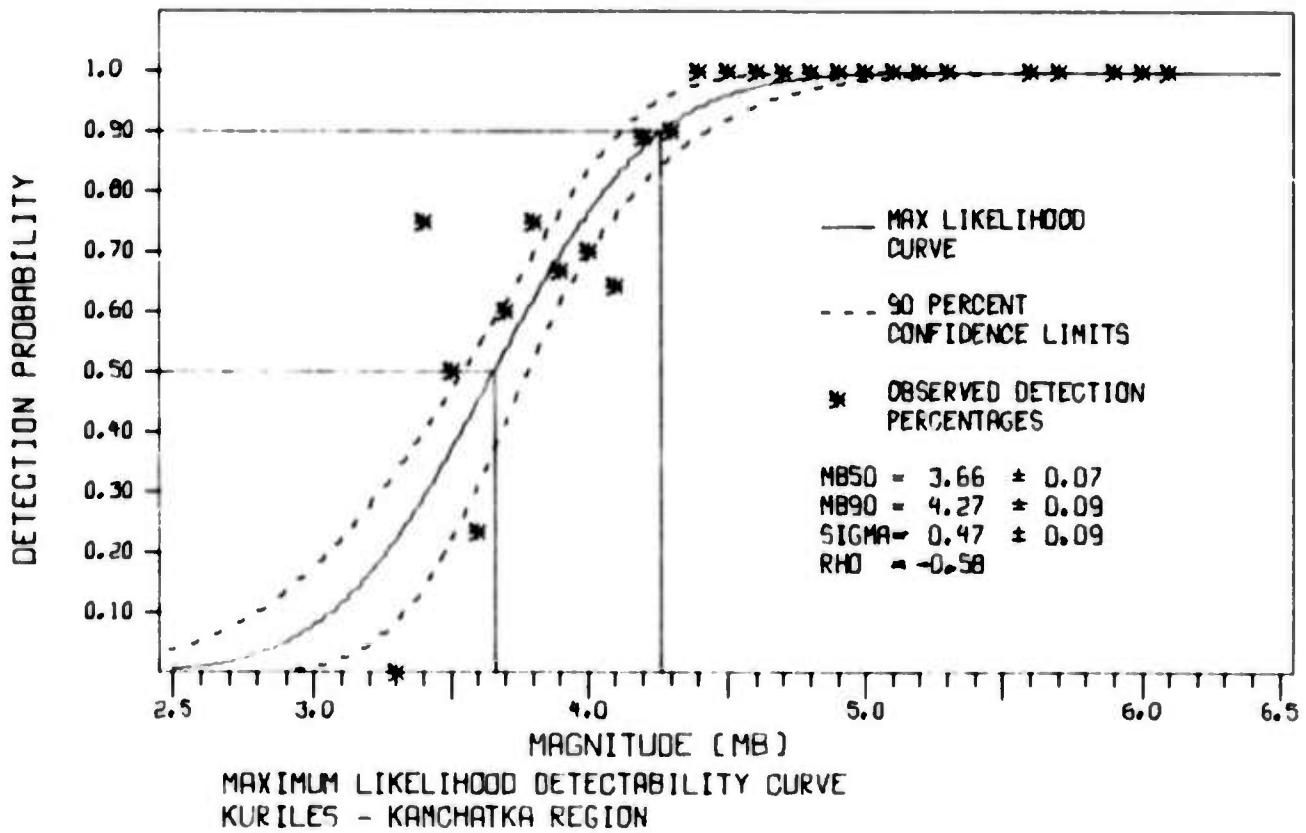
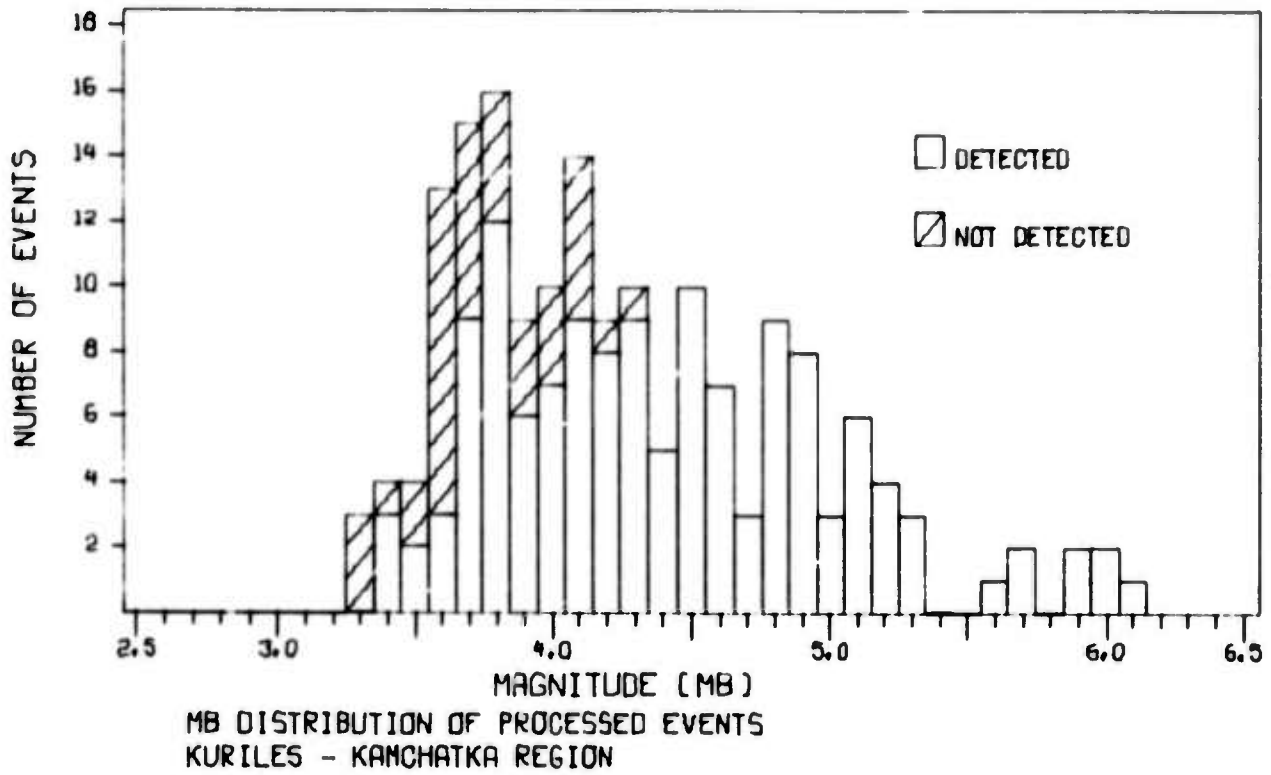
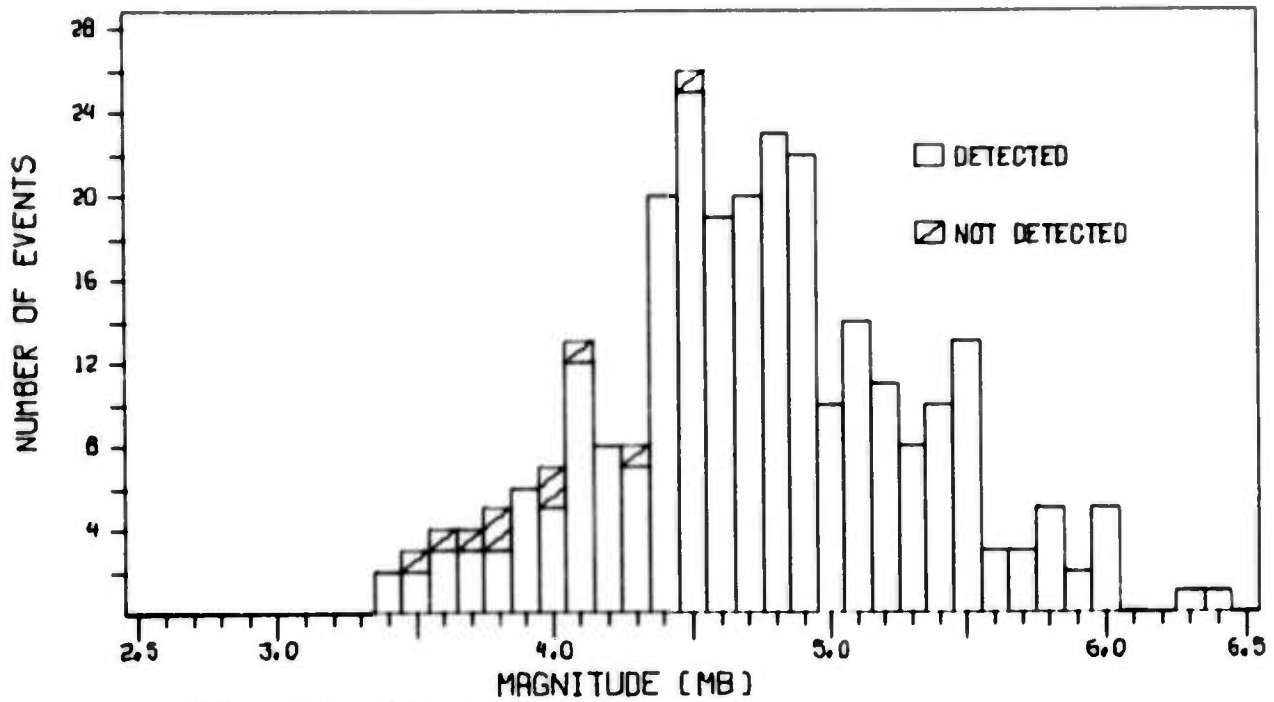
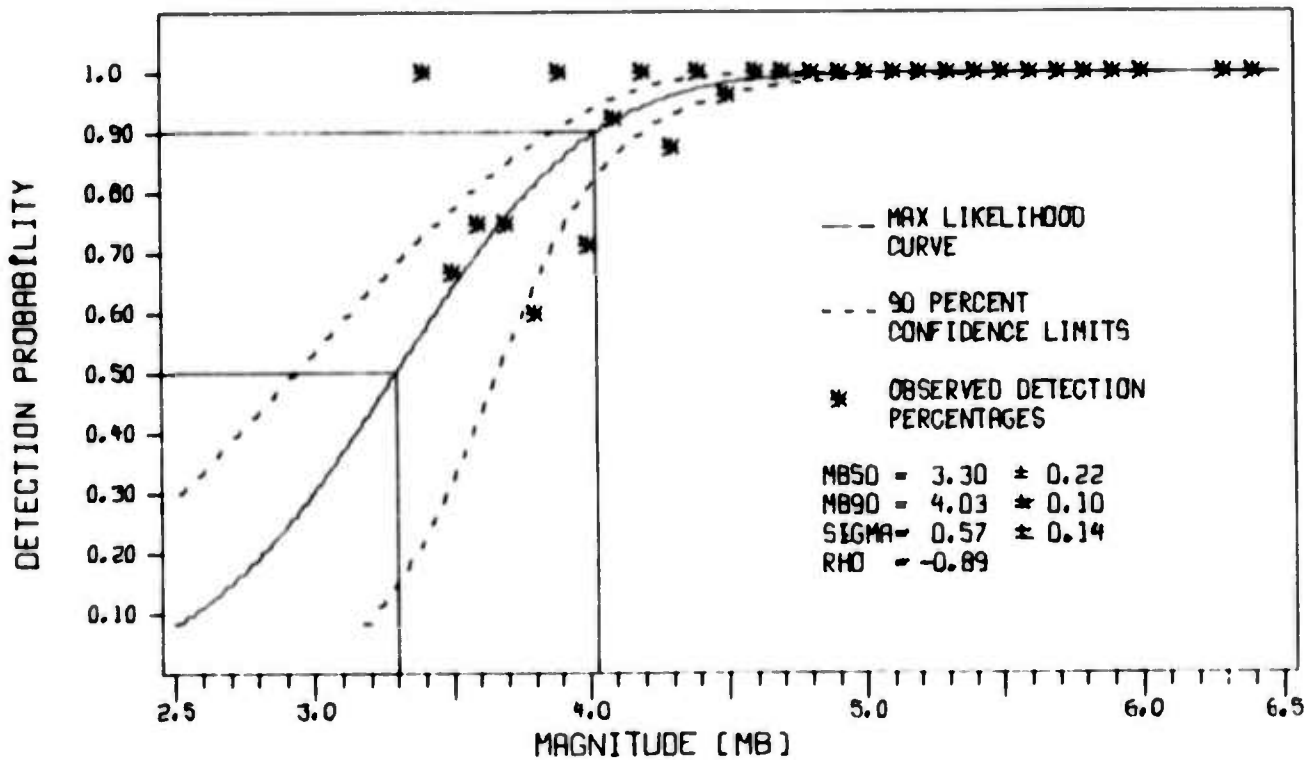


FIGURE IV-1

DIRECT MAXIMUM LIKELIHOOD ESTIMATION OF THE NORSAR, SP
DETECTION CURVE FOR THE KURILES-KAMCHATKA REGION



MB DISTRIBUTION OF PROCESSED EVENTS
EURASIA APART FROM KURILES-KAMCHATKA



MAXIMUM LIKELIHOOD DETECTABILITY CURVE
EURASIA APART FROM KURILES-KAMCHATKA

FIGURE IV-2

DIRECT MAXIMUM LIKELIHOOD ESTIMATION OF THE NORSAR SP
DETECTION CURVE FOR EURASIA APART FROM KURILES-KAMCHATKA

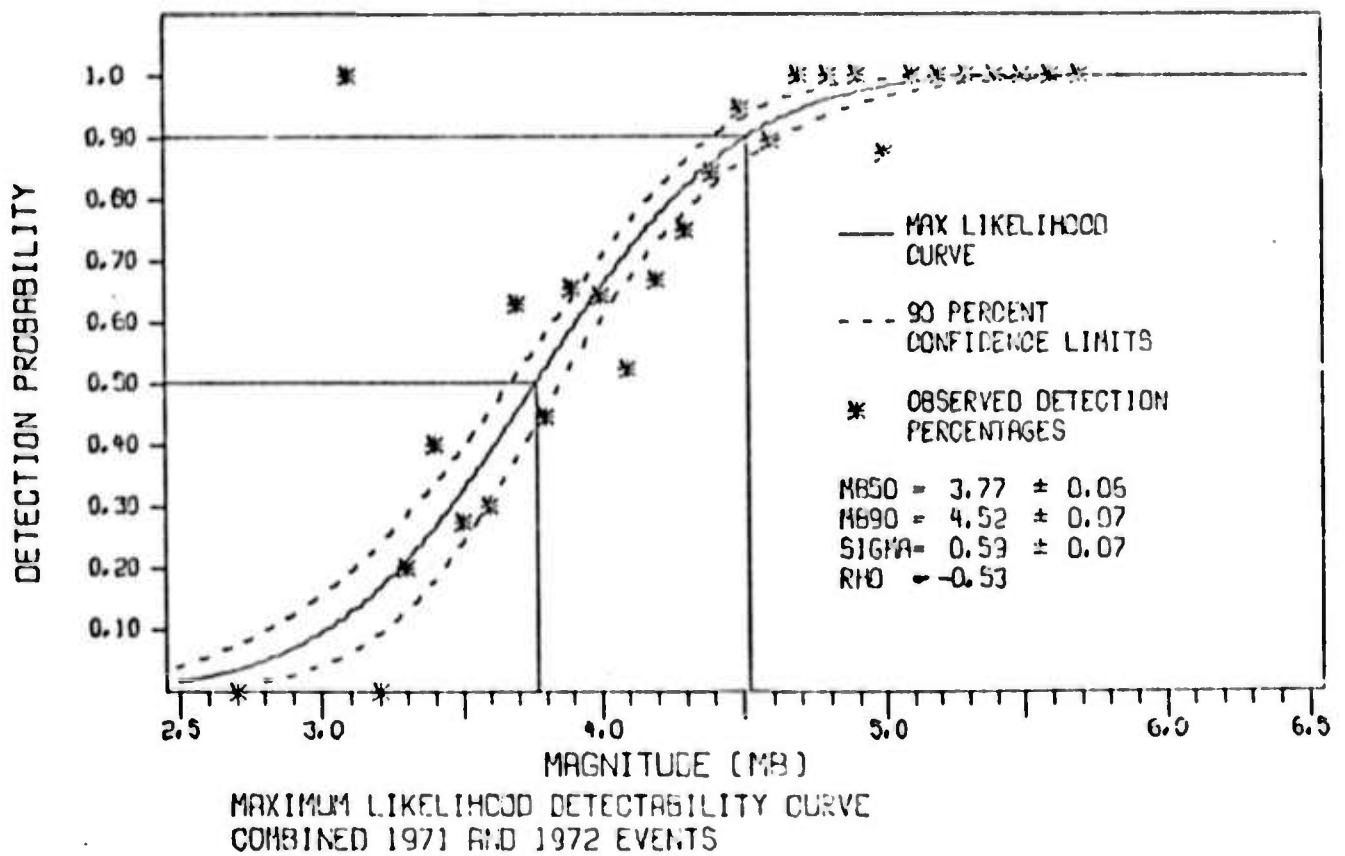
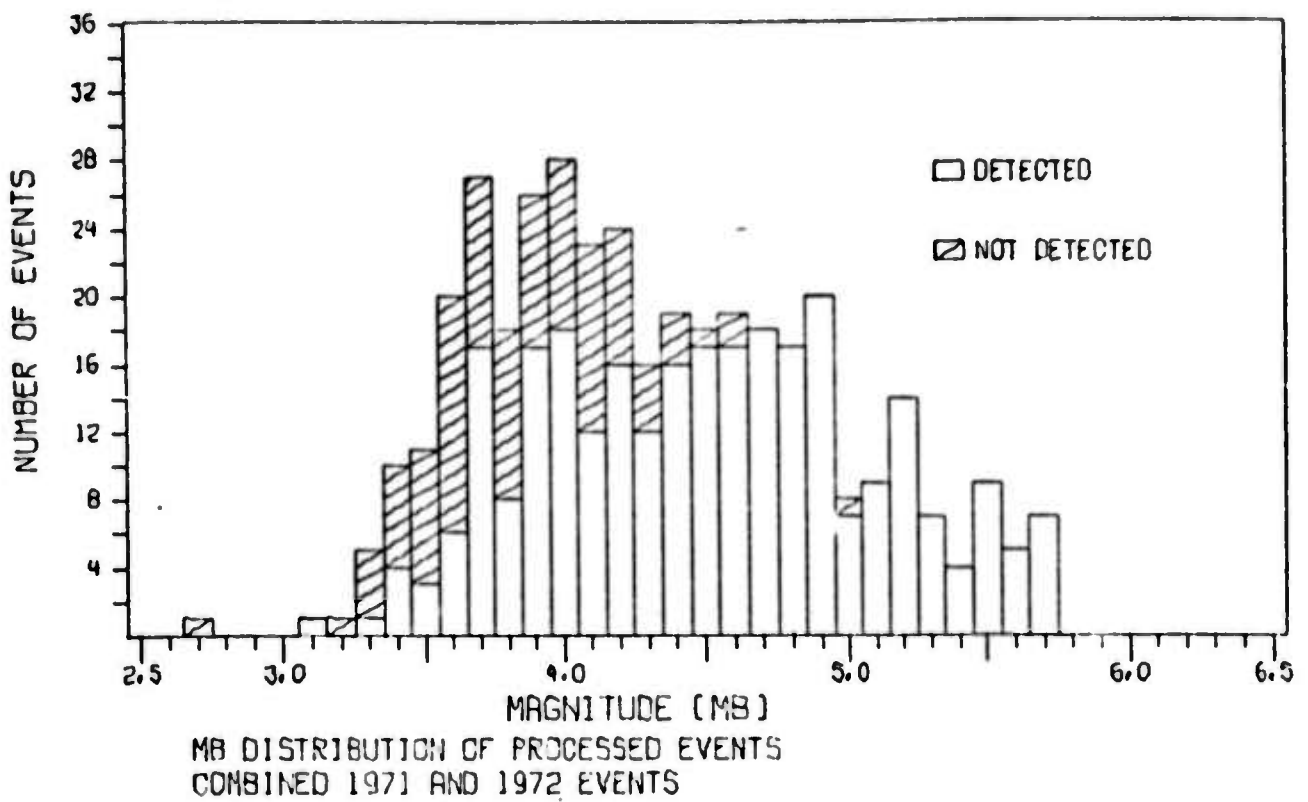


FIGURE IV - 3

DIRECT MAXIMUM LIKELIHOOD ESTIMATION OF THE NORSAR LP
DETECTION CURVE FOR EURASIA

It was obviously necessary to eliminate presumed explosions from the event ensemble in this case, since their $M_s - m_b$ relationship is functionally different from that of earthquakes.

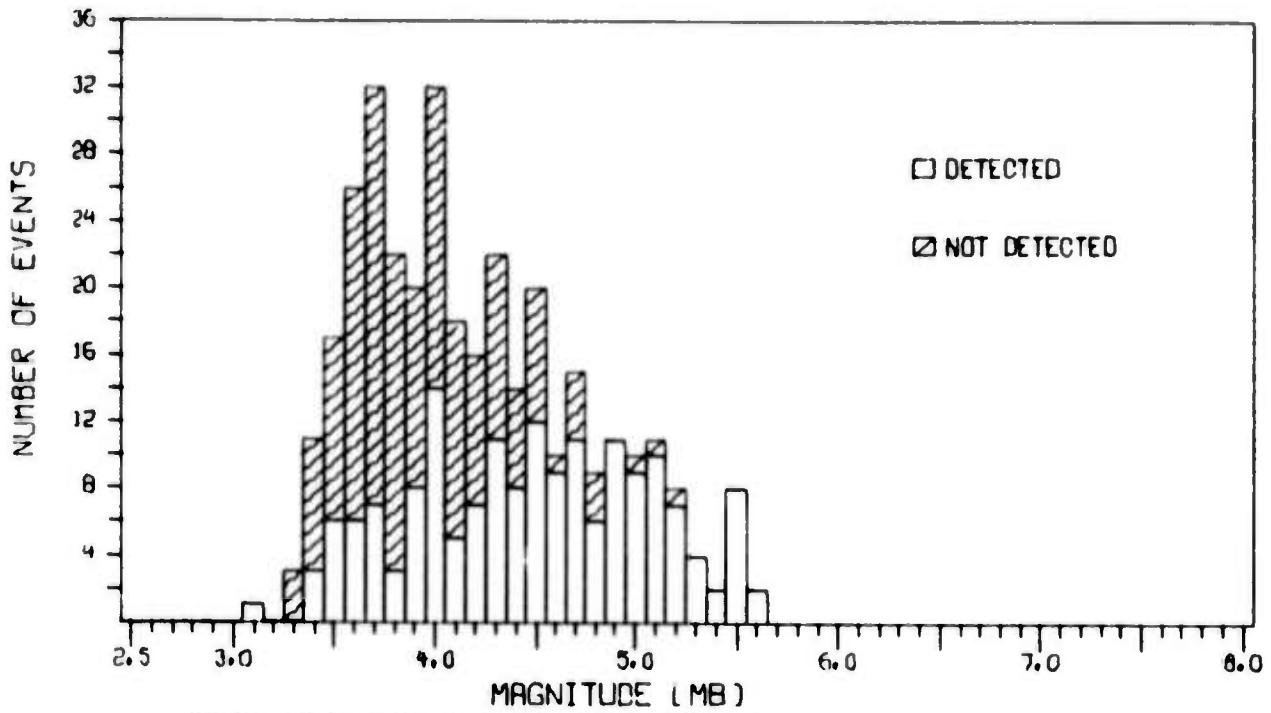
3. VLPE Network Detection Threshold

Our final example concerns the estimation of the network detection capability of the Very Long Period Experiment stations during the winter of 1972. Figure IV-4 is taken from Lambert et. al., (1973), and shows the Eurasian LP detection capability for a network of 6 stations as a function of bodywave magnitude.

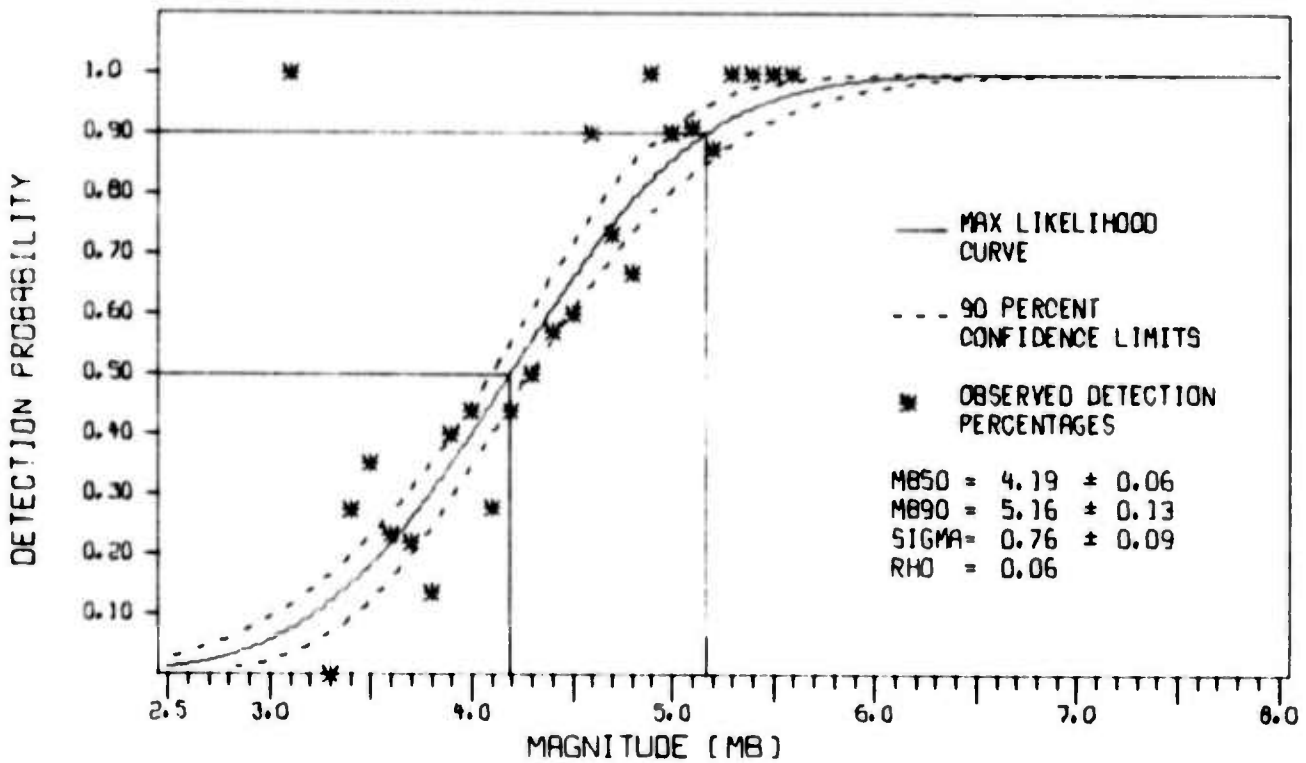
In view of the considerations from Section II, it is reasonable to ask whether the expected lack of symmetry in the theoretical network detection curve has adversely affected the threshold estimates. To investigate this, we performed a series of estimation procedures for subsets of the original reference event set, and the results are shown in Table IV-1. It is seen from this table that by ignoring reference events of low magnitudes, the 50 percent threshold estimate tends to increase slightly, while the 90 percent estimate decreases. This trend is fairly stable up to a cutoff point α about $m_b = 4.5$; if more events are eliminated, the reliability of the estimates decreases sharply due to the low number of non-detections.

Thus we conclude that one must show caution when applying the Gaussian model to a network situation. If one is primarily interested in the 90 percent threshold, a possible approach would be to use the Gaussian model to estimate the upper part of the detection curve, by ignoring low magnitude reference events. It would seem reasonable to choose a cutoff point somewhere around the 50 percent detection threshold in that case.

It should be added that theoretical considerations in this particular case are further aggravated by the failure of stations within the VLPE



MB DISTRIBUTION OF PROCESSED EVENTS
VLPE NETWORK 2



MAXIMUM LIKELIHOOD DETECTABILITY CURVE
VLPE NETWORK 2

FIGURE IV-4

DIRECT MAXIMUM LIKELIHOOD ESTIMATION OF A
VLPE NETWORK DETECTION CURVE

TABLE IV-1
 RESULTS FROM DIRECT MAXIMUM LIKELIHOOD ESTIMATION
 USING VARIOUS SUBSETS OF THE REFERENCE EVENT SET
 (VLPE NETWORK 2, GAUSSIAN MODEL)

Subset of Reference Events Selected	Number of Events	Estimate of μ	Estimate of σ	Estimate of μ_{90}
All events	341	4.19 ± .06	0.76 ± .09	5.17 ± .13
All events of $m_b \geq 3.5$	326	4.20 ± .05	0.71 ± .08	5.12 ± .12
All events of $m_b \geq 3.7$	283	4.24 ± .05	0.62 ± .08	5.05 ± .11
All events of $m_b \geq 3.9$	229	4.22 ± .06	0.65 ± .10	5.06 ± .12
All events of $m_b \geq 4.1$	177	4.32 ± .06	0.52 ± .09	4.99 ± .10
All events of $m_b \geq 4.3$	143	4.30 ± .10	0.54 ± .13	5.00 ± .11
All events of $m_b \geq 4.5$	111	4.29 ± .18	0.55 ± .18	5.00 ± .11
All events of $m_b \geq 4.7$	81	4.41 ± .24	0.47 ± .21	5.02 ± .10
All events of $m_b \geq 4.9$	57	3.83 ± 1.52	0.80 ± .95	4.86 ± .35
All events of $m_b \geq 5.1$	36	4.57 ± .71	0.41 ± .45	5.10 ± .19

network to remain operational during the entire time frame. Thus, for a significant part of the time, only one of the six VLPE stations was operational; while the most typical situation was two or three stations operational (Lambert, et al., 1973).

B. COMPARISON OF THE DIRECT AND INDIRECT ESTIMATION METHODS

As was stated in Section II, the direct and indirect estimation methods estimate different detection curves, so that different results must be expected. In the following we will try to verify the considerations from Section II by applying the two methods to identical test situations and compare the results.

Two large aftershock sequences were selected for this purpose; one from South of Honshu, Japan December 3-20, 1972 and one from Kurile Islands/Hokkaido region June 17-30, 1973. We chose to estimate the operational detection capability for the NORSAR array by the two methods for each aftershock sequence, and compare the results. Thus we considered an event as being detected by NORSAR provided it had been reported in the NORSAR seismic event summary compiled at Kjeller, Norway. It should be noted that swarm situations cannot be considered as typically representing natural seismic activity. Nevertheless, we have found these two examples useful to illustrate the theoretical considerations presented earlier.

1. Direct Estimation

A direct estimation of the NORSAR operational detection threshold for these two aftershock sequences was carried out by Ringdal and Whitelaw (1973b). They used the SDAC/LASA bulletin as a reference, and thus checked each event reported by SDAC/LASA to see if NORSAR had a corresponding detection. Time intervals when the NORSAR array was out of operation were not considered. Thus the total reference data base was 194 events for the Honshu swarm and 364 events for the Kuriles swarm (Table IV-2). Out of these, NORSAR detected 106 and 284 events, respectively.

TABLE IV-2

NORSAR AND LASA EVENT DETECTION PERFORMANCE FOR EARTHQUAKE
 SWARMS FROM SOUTH HONSHU (DECEMBER 3-20, 1972)
 AND THE KURILE ISLANDS (JUNE 17-30, 1973)

	Honshu Swarm	Kuriles Swarm
Distance from NORSAR (degrees)	78	70
Distance from LASA (degrees)	80	69
LASA total detected events	192	364
NORSAR total detected events	133	452
Common events	106	284

Figures IV-5 and IV-6 show the distributions by magnitude (LASA m_b values) of the events detected and not detected, together with the resulting maximum likelihood detection curves. Two important differences may be observed:

- The NORSAR array has significantly better detectability for the Kuriles swarm than for the Honshu swarm. This reflects a much lower seismic noise level at NORSAR during June 1973 than during December 1972.
- The Kuriles detection curve has a significantly larger spread than the Honshu curve ($\sigma = 0.47$ to $\sigma = 0.31$).

This significant difference in values of σ is a very interesting point by itself, and gives us an opportunity to verify one of the basic assumptions of the model described in Section II. According to equation (II-12) of that section, the variance of the detection curve is given by

$$\sigma^2 = \sigma_T^2 + \sigma_N^2 + \sigma_L^2 \quad (IV-1)$$

where σ_T denotes the standard deviation of the "threshold magnitude" while σ_N and σ_L are the standard deviations of the NORSAR and LASA magnitudes, respectively, relative to a hypothetical true magnitude.

In order to evaluate the individual terms of equation (IV-1), we first examined the variations in seismic noise level at NORSAR within the time period covering each event swarm. It was found that the noise level remained essentially constant in both cases, so that σ_T would be relatively insignificant. A value of $\sigma_T = 0.15$ would be about right in both cases.

The next step was to estimate σ_N and σ_L . For this purpose, we selected randomly 50 events from each aftershock sequence, and plotted

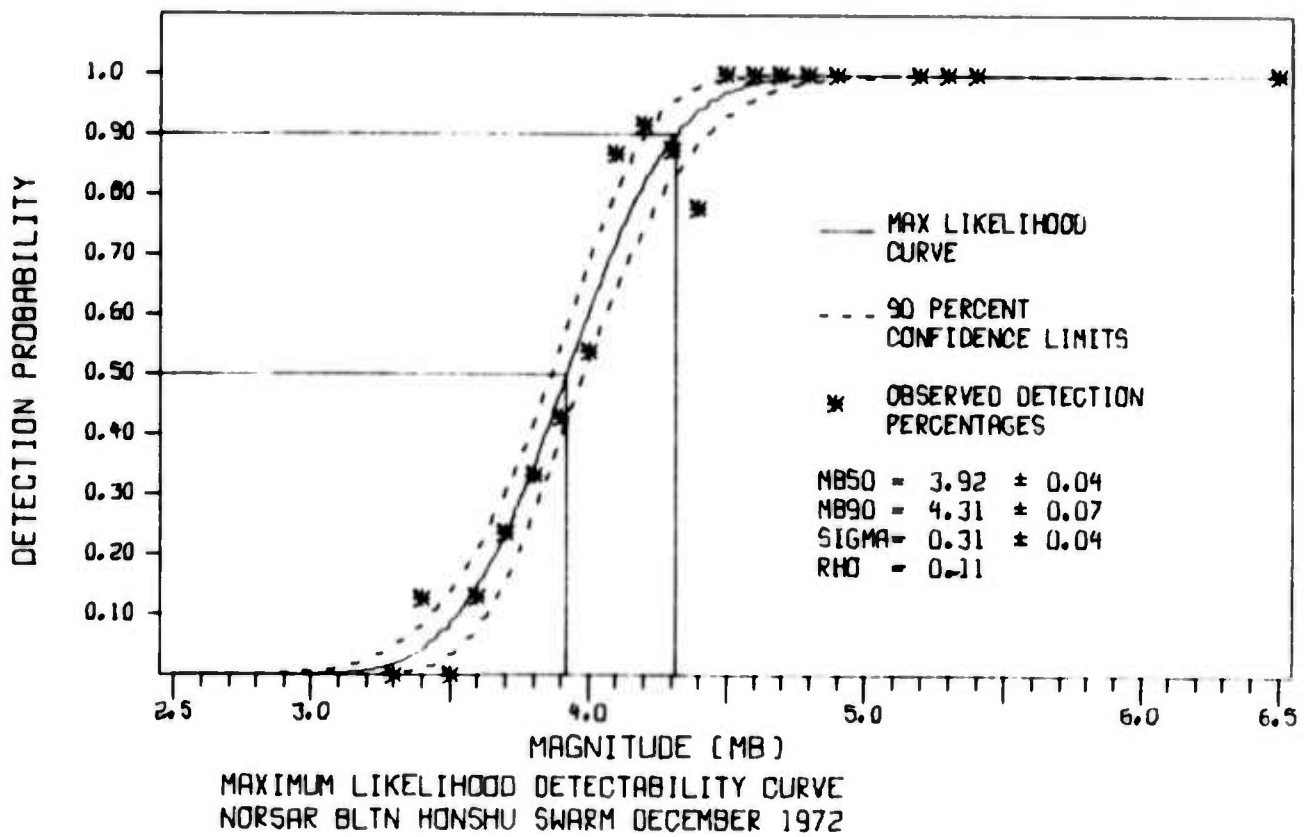
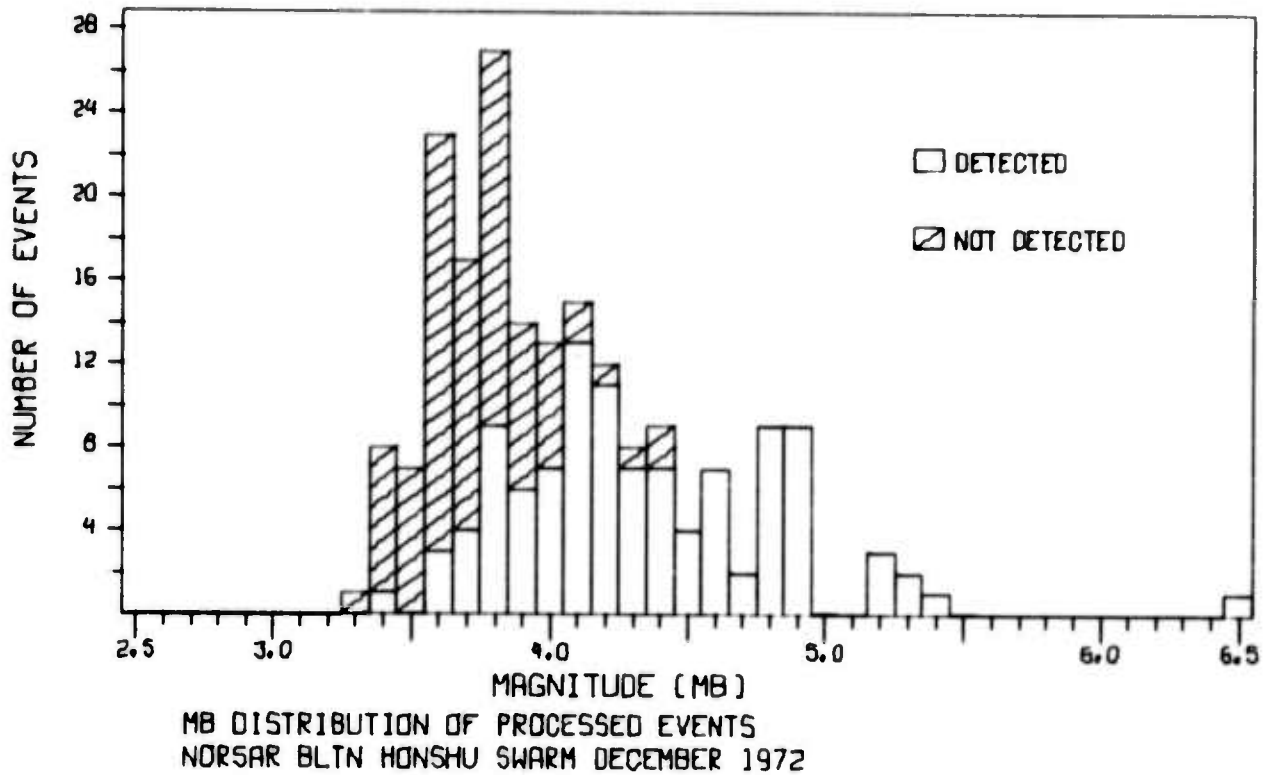
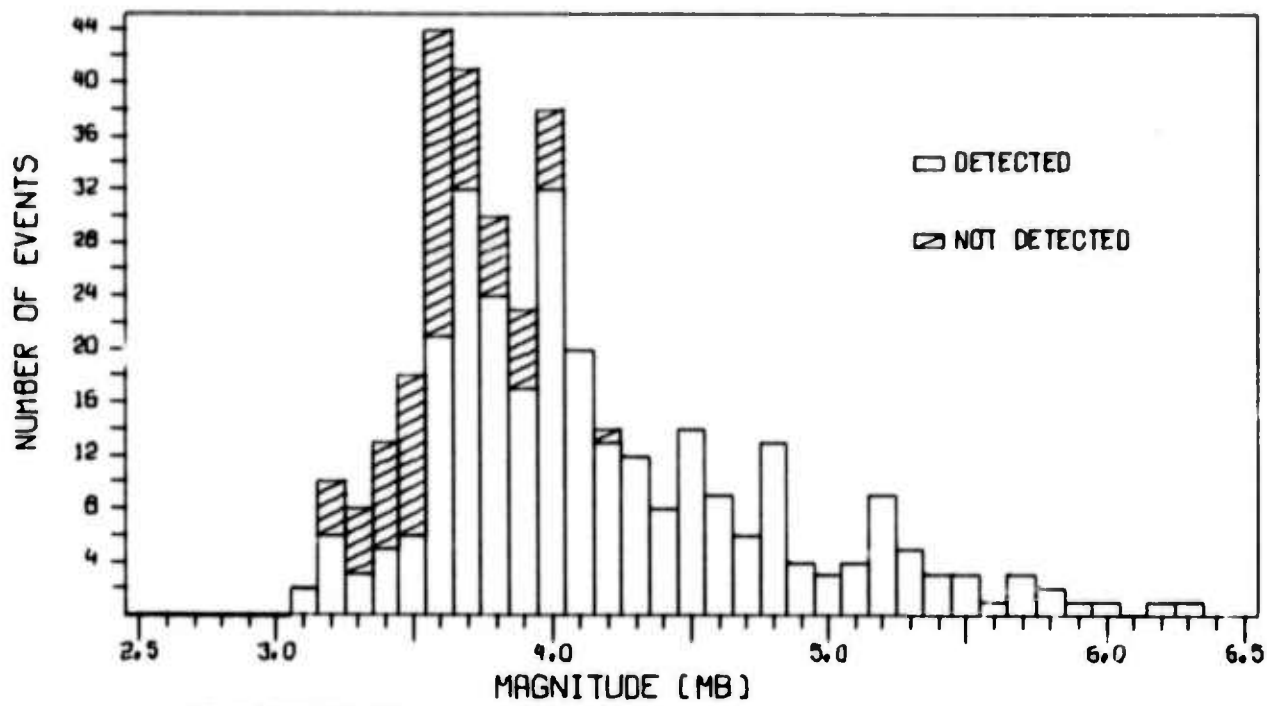
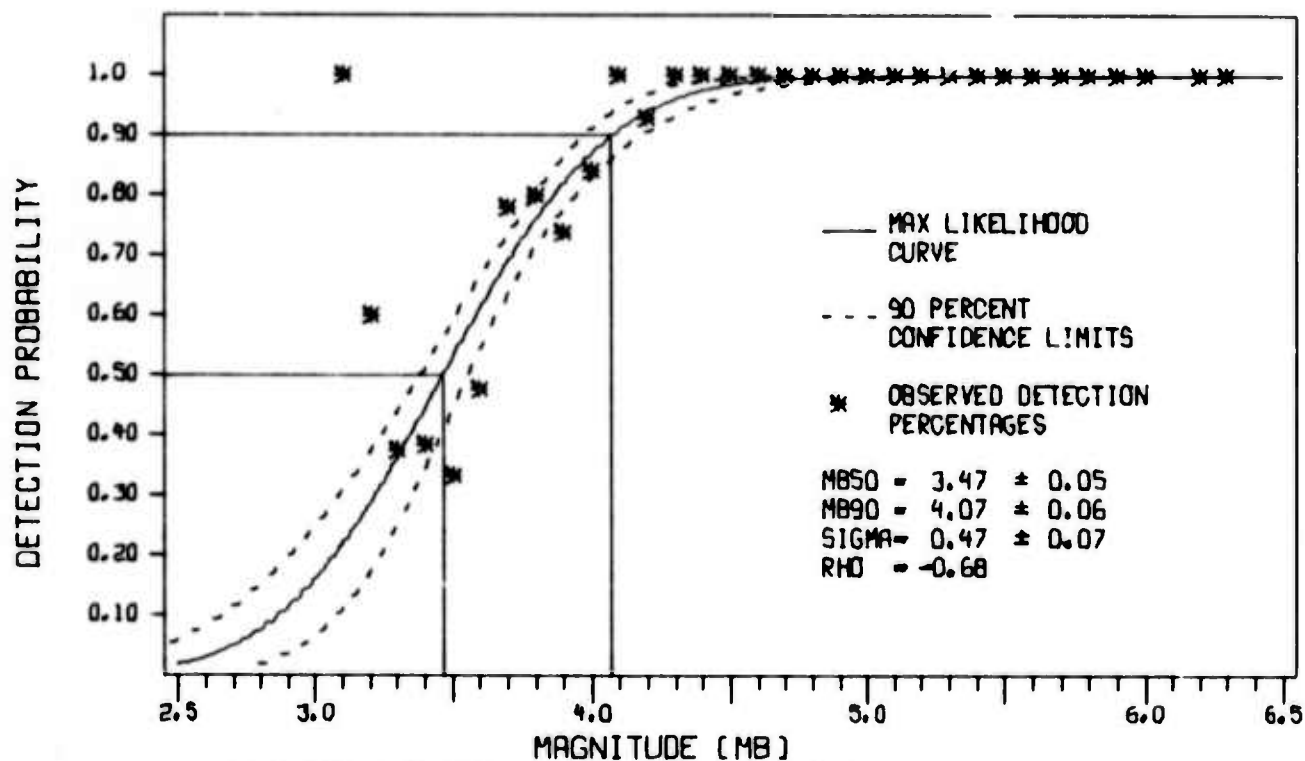


FIGURE IV-5

DIRECT MAXIMUM LIKELIHOOD ESTIMATION OF THE OPERATIONAL
NORSAR SP DETECTION CURVE FOR AN AFTERSHOCK SEQUENCE
FROM SOUTH OF HONSHU



MB DISTRIBUTION OF PROCESSED EVENTS
NORSAR BLTN KURILES SWARM JUNE 1973



MAXIMUM LIKELIHOOD DETECTABILITY CURVE
NORSAR BLTN KURILES SWARM JUNE 1973

FIGURE IV-6
DIRECT MAXIMUM LIKELIHOOD ESTIMATION OF THE OPERATIONAL
NORSAR SP DETECTION CURVE FOR AN AFTERSHOCK SEQUENCE
FROM THE KURILE ISLANDS

NORSAR m_b against LASA m_b as shown in Figures IV-7 and IV-8. We actually selected the first 50 events reported by PDE of $m_b > 4.0$ in each case; for our purpose PDE can be considered to be independent of LASA and NORSAR. Events occurring when one array was out of operation were disregarded. A total of four events (marked as asterisks) were not detected by both LASA and NORSAR; the "missing" magnitudes were then set equal to the apparent "threshold magnitude". The slight bias introduced by this procedure should not be significant.

The most striking observation from Figures IV-7 and IV-8 is the much larger spread between NORSAR and LASA magnitudes in the latter case, which corresponds to the Kuriles swarm. The observed standard deviations are 0.25 and 0.40, respectively. Because of the randomness in event selection, it is clear that, with the notation in the figures:

$$\sigma^2(m_N - m_L) = \sigma_N^2 + \sigma_L^2 \quad (\text{IV-2})$$

so that we obtain an immediate estimate of the remaining terms of equation (IV-1).

Inserting the above numbers in equation (IV-1) we obtain values of $\sigma = 0.29$ for the Honshu swarm and $\sigma = 0.43$ for the Kuriles swarm, which compare well to the respective values of 0.31 and 0.47 estimated by the maximum likelihood method.

The important conclusion from the preceding considerations is not so much the numerical results, but rather the fact that there is a direct connection between the spread in magnitude distribution and the spread in the station detection curve as estimated by the direct method. It would appear that the large spread in the Kuriles magnitude ensemble reflects a greater variation in source mechanisms for this event set than among the Honshu aftershocks.

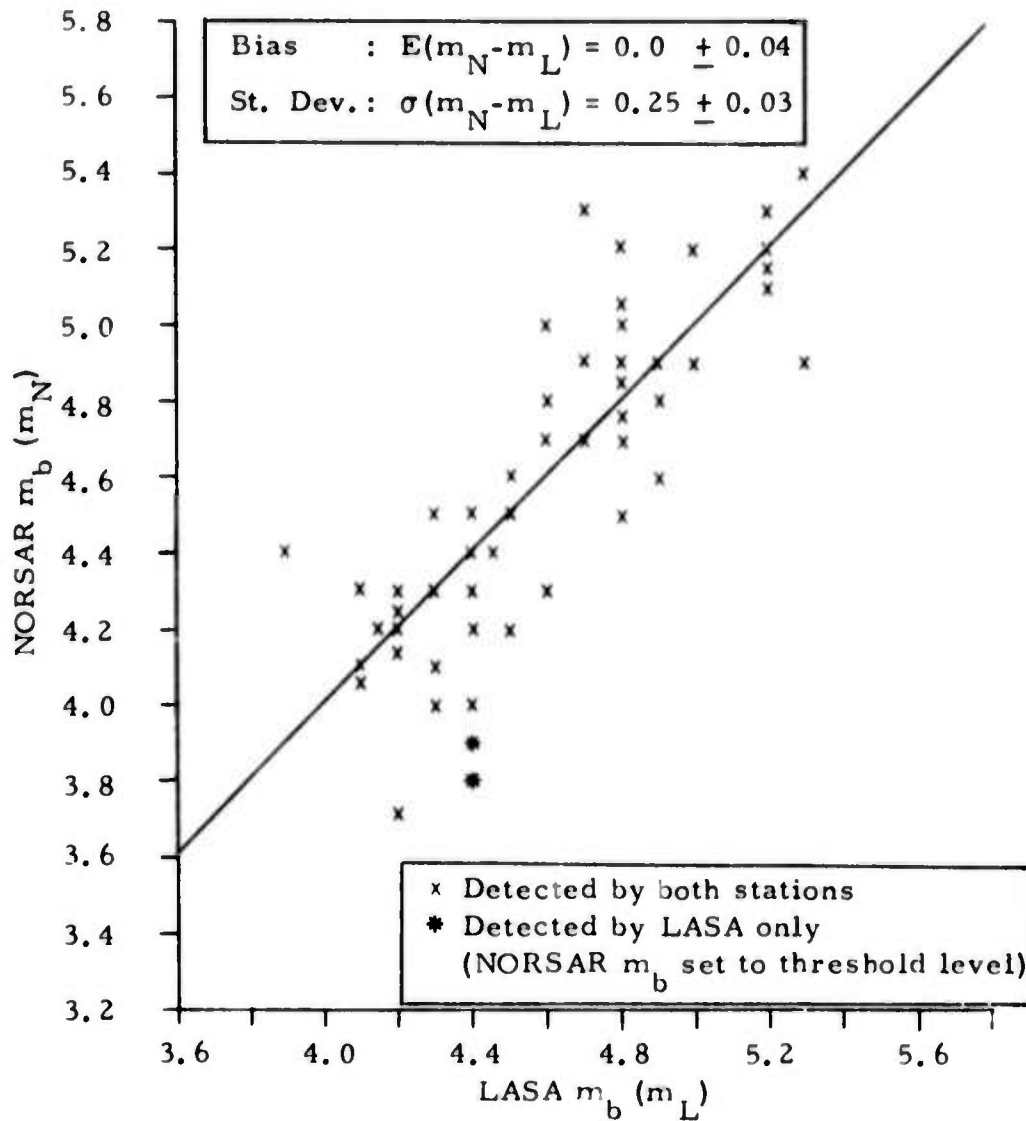


FIGURE IV-7

NOR SAR m_b VERSUS LASA m_b FOR 50 EVENTS RANDOMLY SELECTED FROM THE SOUTH HONSHU AFTERSHOCKS

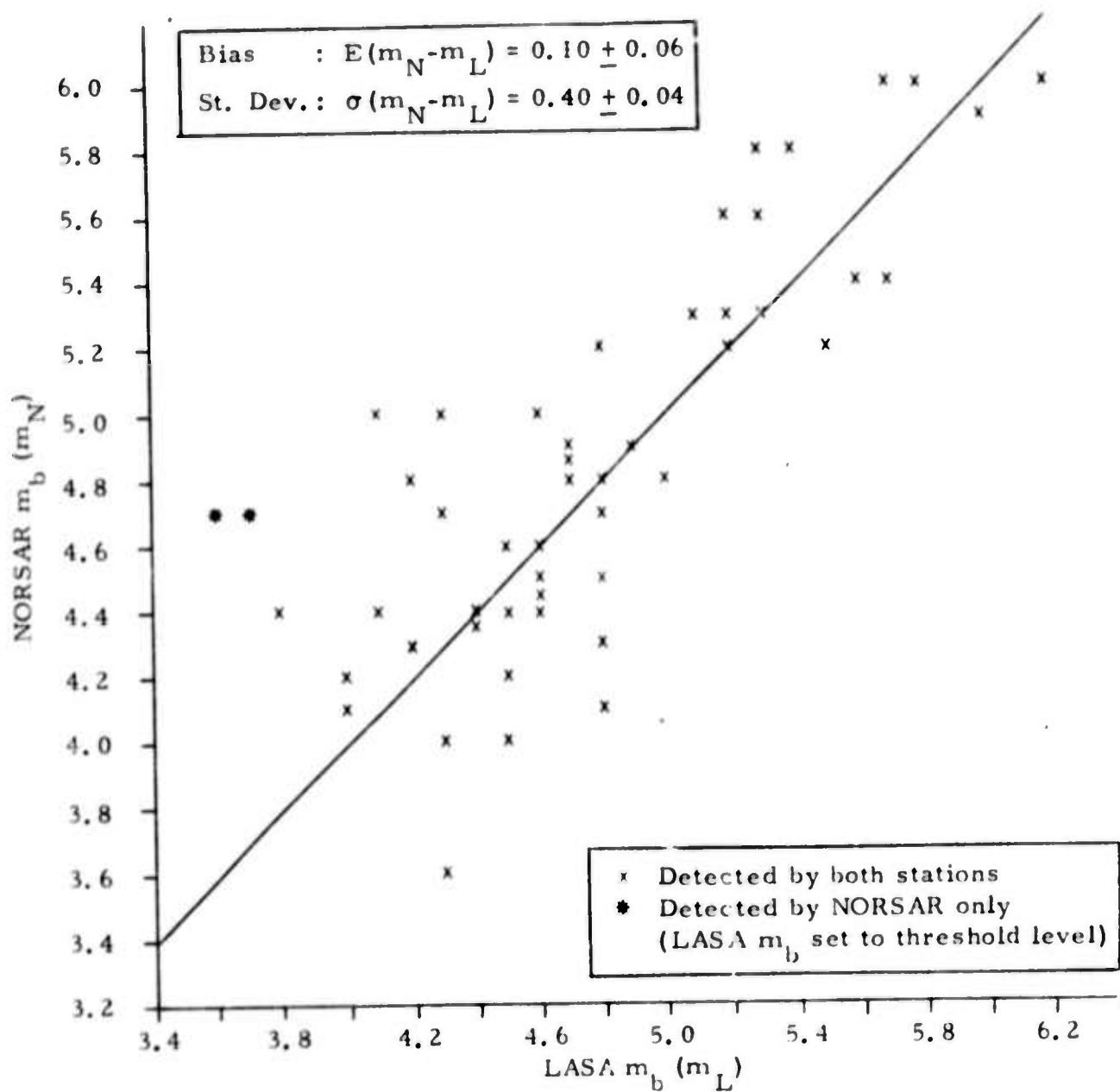


FIGURE IV-8

NOR SAR m_b VERSUS LASA m_b FOR 50 EVENTS RANDOMLY SELECTED FROM THE KURILE ISLANDS AFTERSHOCKS

2. Indirect Estimation

The indirect maximum likelihood method was also applied to the two aftershock sequences described previously. The number of events reported in the NORSAR bulletin in each case is shown as a function of magnitude in the histograms of Figures IV-9 and IV-10. These figures correspond to the Honshu swarm and the Kuriles swarm, respectively. Since NORSAR did not report a magnitude for the main shock of the Honshu swarm (due to system saturation), the LASA magnitude for this event was used instead.

The two figures also list the estimated seismicity parameters and the parameters of the detection curves. The incremental seismicity $n(m)$ which is given by

$$n(m) = b \cdot e^{a-bm} \quad (\text{IV-3})$$

is shown as a dashed curve. A curve showing the (incremental) expected number of detections $E(m)$ is also drawn. This curve is specified by

$$E(m) = n(m) \cdot P(m) \quad (\text{IV-4})$$

where $P(m)$ is the estimated detection probability for an event of magnitude m . The "goodness of fit" of this curve to the histogram is an indication as to how well the theoretical model with the estimated parameters actually fits the experimental data. We observe that the fit appears to be quite good in both cases.

Confidence limits have not been computed for the indirect estimates. However, an idea about the confidence of the estimates of the Honshu swarm can be obtained from the simulation experiment in Subsection III-D, which dealt with a very similar situation. The confidence in the parameter values for the Kuriles swarm should be somewhat better, since the number of events is higher by a factor of three.

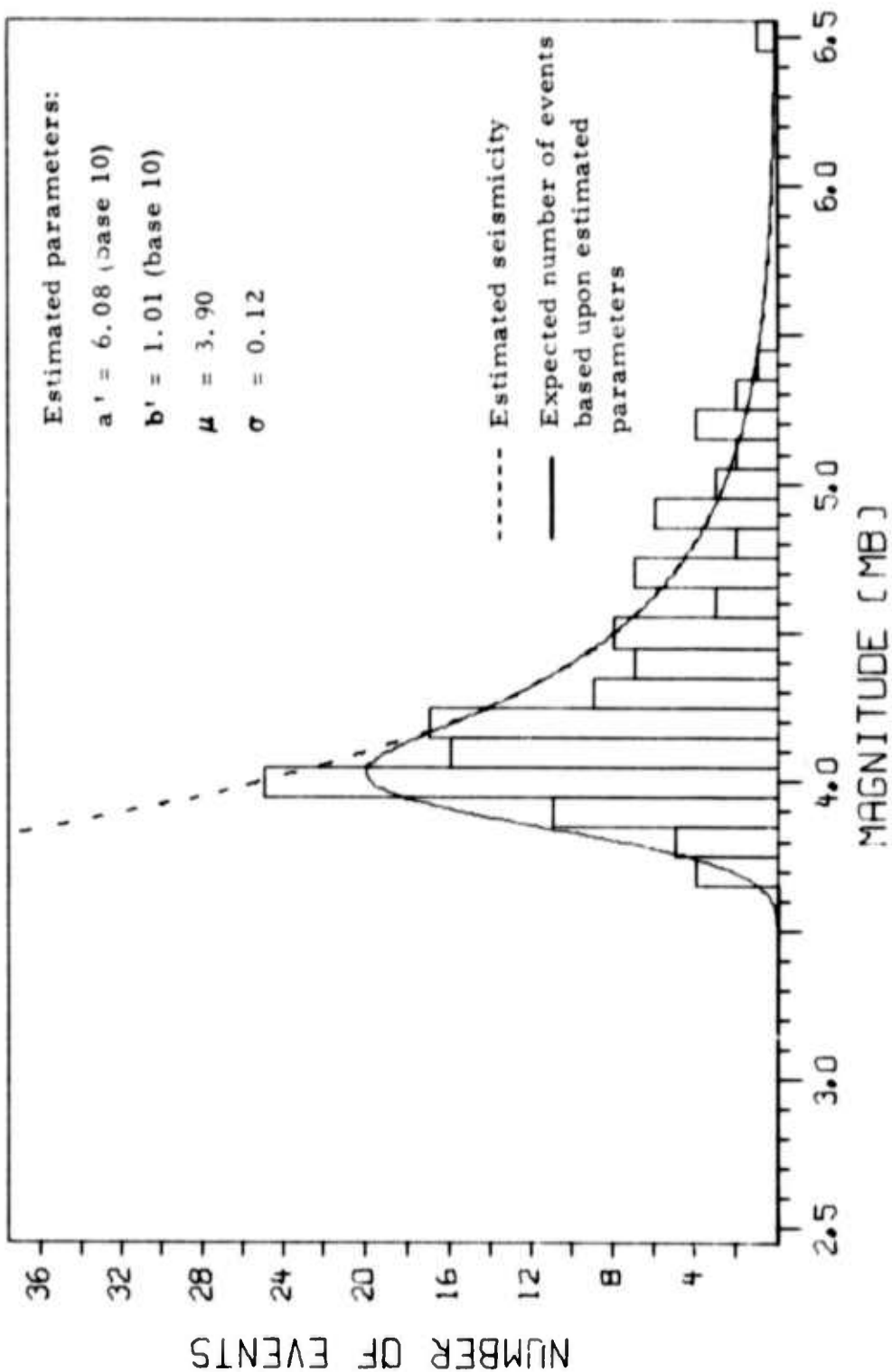


FIGURE IV-9
 DETECTION STATISTICS FOR THE INDIRECT MAXIMUM LIKELIHOOD METHOD
 APPLIED TO NORSAR SP OPERATIONAL PERFORMANCE FOR THE SOUTH
 HONSHU AFTERSHOCK SEQUENCE

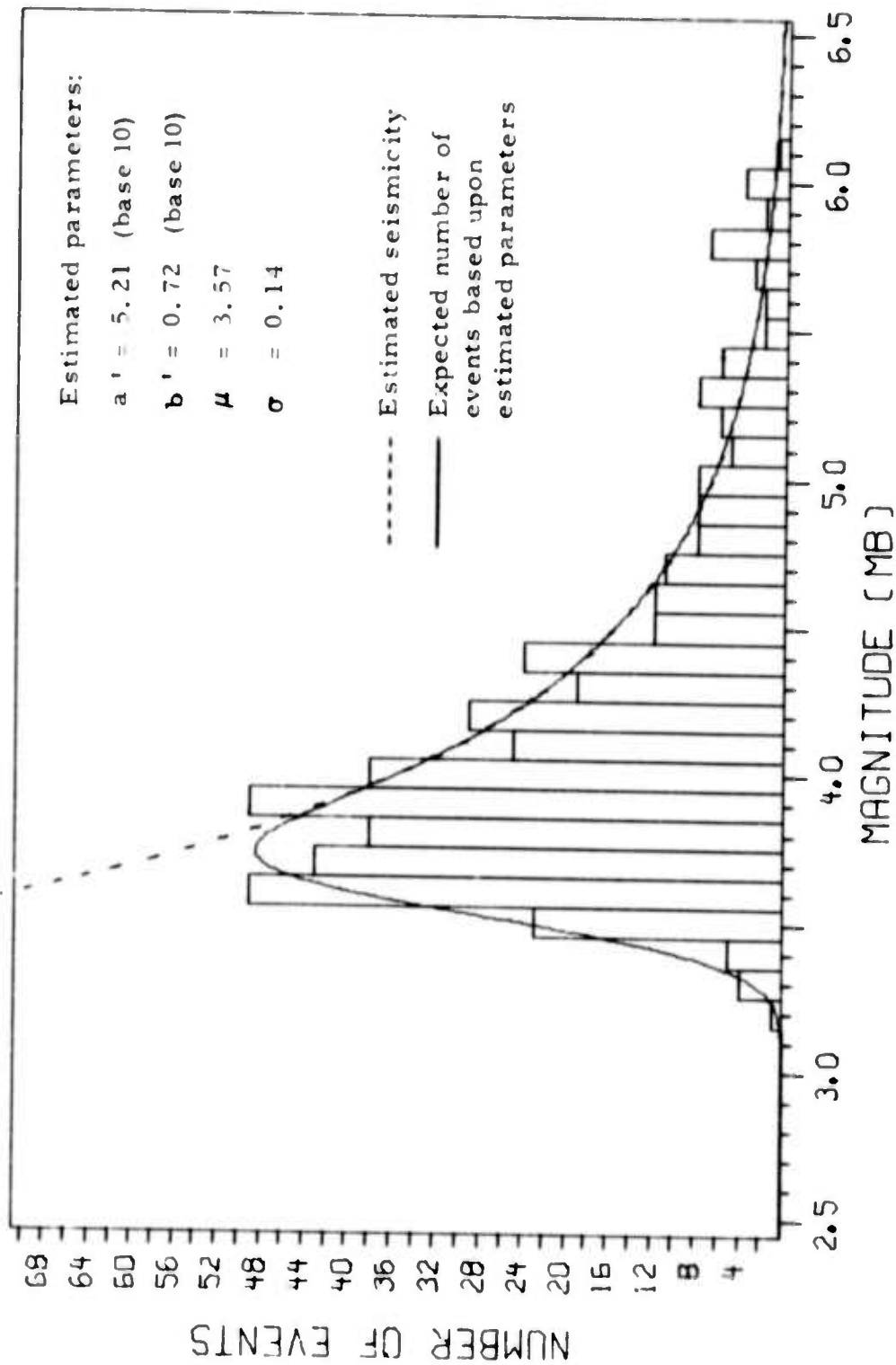


FIGURE IV-10

DETECTION STATISTICS FOR THE INDIRECT MAXIMUM LIKELIHOOD METHOD
 APPLIED TO NORSAR SP OPERATIONAL PERFORMANCE FOR THE KURILE
 ISLANDS AFTERSHOCK SEQUENCE

3. Comparison of Results

The estimated parameter values by the two methods (μ , σ and 90 percent threshold μ_{90}) are summarized in Table IV-3. The following observations may be noted:

- The parameter σ estimated by the indirect method is significantly lower in both cases (0.12 versus 0.31 and 0.14 versus 0.47, respectively). This is in excellent agreement with our considerations in Section II, equations (II-7) and (II-12), which imply that the indirect method estimates the variation σ_T in the threshold magnitude only, and does not relate to the signal variations σ_N and σ_L .
- As expected from the above observation, the 90 percent detection thresholds estimated by the indirect method are much lower than the direct estimates in both cases (0.25 and 0.4 m_b units, respectively). In fact, our considerations in Section II imply that the "true" 90 percent threshold is somewhere between the direct and indirect estimates.
- The 50 percent detection threshold μ is about the same in the two cases, after compensating for the bias between NORSAR and LASA magnitudes for the Kuriles swarm. We had actually expected the direct estimates to be higher by an amount of $b\sigma_L^2$ (Figure II-2); i.e., about 0.07 m_b units for the Honshu swarm and 0.13 m_b units for the Kuriles swarm. However, these deviations are within the uncertainties of the mathematical model.

In conclusion, we again stress that the important point is not so much the numbers involved, but rather the fact that the direct and indirect methods estimate two different detection curves, and that the resulting estimates

TABLE IV-3
 COMPARISON BETWEEN DETECTION PARAMETER ESTIMATES
 OBTAINED BY THE DIRECT AND INDIRECT METHODS FOR
 THE NORSAR SP OPERATIONAL PERFORMANCE FOR
 TWO AFTERSHOCK SEQUENCES

	Honshu Swarm			Kuriles Swarm		
	μ	σ	μ_{90}	μ	σ	μ_{90}
Estimates by the direct method	3.92	0.31	4.31	3.47	0.47	4.07
Estimates by the indirect method	3.90	0.12	4.06	3.57*	0.14	3.75*

* Note that the NORSAR-LASA m_b bias of 0.10 should be subtracted from these values in order to make them compatible with the direct estimates.

of threshold parameters must be interpreted accordingly. In our opinion, the failure of the indirect method to take the signal variation into account is a serious drawback with this estimation technique.

SECTION V

SUMMARY AND CONCLUSIONS

The first topic of this report was to define the detection curve of a seismic station or network as the probability of detection as a function of event magnitude. The following observations were made:

- Under reasonable assumptions, the detection curve of a single station (or seismic array) for a limited region can be approximated by a cumulative Gaussian distribution function. In this Gaussian model, then, the parameters μ and σ of the distribution completely define the detection curve.
- The Gaussian model does not theoretically apply to seismic networks, but may still be useful as an approximation to the network detection curve within limited magnitude ranges.
- A very important observation is that the detection curve of a seismic system varies with the choice of reference magnitudes. Thus a detection curve estimated from a station's own magnitudes tends to give a significantly lower 90 percent detection threshold than if a different station's magnitudes are chosen as reference.

A maximum likelihood method for estimating the detection capability of a seismic station or network in terms of magnitudes from an independent reference system was presented. The method is based upon a direct verification of detection or no detection for a set of reference events. Our presentation can be summarized as follows:

- The likelihood function for the method was derived and asymptotic confidence limits for the estimated parameters were computed.
- A simulation experiment showed that the asymptotic confidence limits were good indications of the stability of the estimates in a test case with 100 reference events (of which 75 were detected). A test case with 20 reference events (10 detections) indicated that the method should be used only with caution for data samples of this size.
- It was emphasized that the estimation procedure is only as valid as the model. The method is sensitive to "bad" data points, such as a large event that is not detected or a very low magnitude event that is detected. A careful data screening is necessary to eliminate observations that either violate the independence requirement or have questionable reference magnitudes. Thus, as an example, the lack of consistency in PDE m_b estimates suggests that LASA and NORSAR may in many cases be better suited as reference systems than PDE.

A brief description of the indirect maximum likelihood estimation method developed by Lacoss and Kelly (1969) was also included. A simulation experiment showed that this method gave reasonable stable estimates in a test case with an expected number of 133 events. Data screening in this case would be easier than for the direct estimation, and the major concern would be to make appropriate limitations to the seismic region considered, so that the Gaussian model is valid.

Finally, examples of applications were shown, with emphasis on the direct method. For two earthquake aftershock sequences, a comparison was carried out between the direct and indirect estimation method. The result

was found to be in agreement with the theoretical considerations regarding the detection curves.

In conclusion, it is felt that maximum likelihood estimation is a feasible approach to obtaining estimates of the detection thresholds of seismic stations and networks. When choosing between the direct and the indirect methods of estimation, we observe that the latter method has the following two major disadvantages:

- The seismicity estimates by the indirect method are based upon detections by the station itself, and may not always be reliable. For example, suppose we want to estimate the NORSAR operational detection capability for a region with poor beam coverage. The seismicity estimates for this region based on NORSAR detections will then clearly be biased low, thus causing the indirect method to estimate too high detection probabilities.
- The indirect method fails to take the signal variance into account when estimating detection thresholds. Therefore the 90 percent thresholds found by this method will always be significantly lower than the "true" threshold when estimating station detection capability.

For the above reasons, we feel that the direct method of estimation is a superior approach to obtaining reliable detection threshold estimates. This method has the added advantage of giving easy visual control of the results. However, the direct method does require that a good reference network or station be available. In the hypothetical case of a "perfect" reference network, the resulting estimates from the direct method would represent the "true" detection probabilities. In practical situations, the variance of the reference magnitude estimates must be considered when evaluating the results.

As in all applications of statistical estimation theory, it is necessary to do a careful data screening prior to applying the mathematical tools. It is important to remember that the estimators, being random variables, sometimes will produce results that deviate significantly from the true parameter values. Thus, a careful interpretation of the results is required when applying the techniques described in this report.

SECTION VI
REFERENCES

- Alsup, S. A., and E. S. Becker, 1973, Long-Term Broad-Band Vertical Earth Noise Structure at Very Long Period Experiment Sites, Special Report No. 3, Extended Array Evaluation Program, Contract Number F33657-72-C-0725, Texas Instruments Incorporated, Dallas, Texas.
- Barnard, T. E., and R. L. Whitelaw, 1972, Preliminary Evaluation of the Norwegian Short Period Array, Special Report No. 6, Extended Array Evaluation Program Contract Number F33657-71-C-0843, Texas Instruments Incorporated, Dallas, Texas.
- Bungum, H., and E. S. Husebye, 1974, Analysis of the Operational Capabilities for Detection and Location of Seismic Events at NORSAR, Bulletin Seismological Society of America (in press).
- Cramer, H., 1945, Mathematical Methods of Statistics, Princeton University Press, Princeton, New Jersey.
- Evernden, J. F., W. J. Best, P. W. Pomeroy, T. V. McEvelly, J. M. Savino, and L. R. Sykes, 1971, Discrimination between Small-Magnitude Earthquakes and Explosions, Journal of Geophysical Research, 76, 8042-8055.
- Freedman, H. W., 1967, Estimating Earthquake Magnitude, Bulletin Seismological Society of America, 57, 747-760.
- Gerlach, G. S., T. T. Goforth, F. F. Seymour, and J. G. Swanson, 1966, Estimates of the Detection Capability of four VELA-Uniform Seismological Observatories, Technical Report No. 66-1, Teledyne Industries, Goetech Division, Garland, Texas, 369.

- Gutenberg, B., and C. F. Richter, 1956, Magnitude and Energy of Earthquakes, *Annali de Geofisica*, (Rome), 9, 1-15.
- Harley, T. W., and L. N. Heiting, 1972, Indirect Estimates of Surface Wave Detection Probabilities, Special Report No. 1, Extended Array Evaluation Program, Contract Number F33657-72-C-0725, Texas Instruments Incorporated, Dallas, Texas.
- Herrin, E., and W. Tucker, 1972, On the Estimation of Bodywave Magnitude, Technical Report to AFOSR, Dallas Geoph. Lab., SMU, Dallas.
- Lacoss, R. T., 1971, Seismic Event Detection and Discrimination - some Statistical Considerations, NORSAR Seminar, Oslo, Norway.
- Lacoss, R. T., and E. J. Kelly, 1969, Estimation of Seismicity and Network Detection Capability, MIT Lincoln Laboratories Technical Note 41.
- Lambert, D. C., S. R. Prael, and A. C. Strauss, 1973, Evaluation of the Noise Characteristics and the Detection and Discrimination Capabilities of the Very Long Period Experiment (VLPE) Single Stations and the VLPE Network, Special Report No. 14, Texas Instruments Report Number ALEX(01)-STR-73-14, Contract Number F33657-72-C-0725.
- Lanz, A., 1966, Normality of Linear or Logarithmic Data, (unpublished memorandum), Teledyne Industries, Geotech Division, Garland, Texas.
- Laun, P. R., W. W. Shen, and W. H. Swindell, 1973, Evaluation of the Norwegian Long Period Array - Final Report, Special Report No. 12, Texas Instruments Report Number ALEX(01)-STR-73-12, Contract Number F33657-72-C-0725.
- Ringdal, F., and R. L. Whitelaw, 1973a, Continued Evaluation of the Norwegian Short Period Array, Special Report No. 9, Extended Array Evaluation Program, Contract Number F33657-72-C-0725, Texas Instruments Incorporated, Dallas, Texas.

Ringdal, F., and R. L. Whitelaw, 1973b, Evaluation of the Norwegian Short
Period Array - Final Report, Special Report No. 11, Texas Instru-
ments Report Number ALEX(01)-STR-73-11, Contract Number
F33657-72-C-0725.

Tsai, Y. B., 1972, Utility of Tsai's Method for Seismic Discrimination,
Semi-Annual Technical Report No. 2, Contract Number F44620-71-
C-0112, Texas Instruments Incorporated, Dallas, Texas.

Veith, K. F., and G. E. Clawson, 1972, Magnitude from Short-Period P-
Wave Data, Bulletin Seismological Society of America, 62, 435-452.

APPENDIX A

STATISTICAL PROPERTIES OF STATION MAGNITUDE DISTRIBUTIONS

We will in the following focus upon some statistical properties of station magnitudes that follow from the assumptions made previously in this report. We will in general not refer to the detection performance of any seismic system during these considerations, thus, we assume that for any seismic event the station magnitude is defined regardless of whether or not a signal is actually detected. To be specific, we will refer to LASA and NOR-SAR station magnitudes as estimates of a hypothetical "true" magnitude. However, the results are clearly valid for other stations or networks that satisfy the basic assumptions.

Our two basic assumptions, as stated in Section 1, are:

- Given that an event has true magnitude $m=x$, then
 - The distribution of the NORSAR magnitude m_N is $N(x + b_N, \sigma_N^2)$
 - The distribution of the LASA magnitude m_L is $N(x + b_L, \sigma_L^2)$
 - The two random variables m_N and m_L are independent.
- The number of earthquakes $N(x)$ exceeding a given true magnitude $m=x$ may be expressed as:

$$N(x) = e^{a-bx} \quad (A-1)$$

1. Distribution of True Event Magnitude Given Station Magnitude

The first topic is to find what can be said about the true magnitude of an event, given e.g., the value of the LASA magnitude m_L of that

event. For this purpose, we find it convenient to consider the true magnitude m as being a random variable, with a certain probability distribution. For example, if we consider all events of true magnitude greater than an arbitrary value m_0 , then the probability density function $w(m)$ of m can be derived from (A-1):

$$w(m) = b \cdot e^{-b(m - m_0)} \quad m \geq m_0 \quad (\text{A-2})$$

The probability density function (A-1) is often referred to as the a priori distribution of m . Our purpose is to find the distribution of m , given that $m_L = x$. This conditional distribution is called the a posteriori distribution of m , given m_L , and we will denote it as $h(m/m_L)$.

Following Cramer (1945) page 508, we obtain:

$$h(m/m_L) = \frac{w(m) \cdot g_L(m_L/m)}{\int_{m_0}^{\infty} w(m) \cdot g_L(m_L/m) dm} \quad ; m \geq m_0 \quad (\text{A-3})$$

where $g_L(m_L/m)$ according to our first basic assumption is a Gaussian probability density function:

$$g_L(m_L/m) = \left(2\pi\sigma_L^2\right)^{-1/2} e^{-\frac{(m_L - (m+b_L))^2}{2\sigma_L^2}} \quad (\text{A-4})$$

When inserting (A-2) and (A-4) in the expression (A-3) we first observe that the term in $w(m)$ involving m_0 cancels. Thus it is evident that the expression (A-3) has a limiting value as $m_0 \rightarrow -\infty$, since the integral in the denominator is convergent. It turns out that this infinite integral can be evaluated, and we obtain after some computation:

$$h(m/m_L) = \left(2\pi\sigma_L^2\right)^{-1/2} \cdot e^{-\frac{(m - (m_L - b_L - b\sigma_L^2))^2}{2\sigma_L^2}} \quad (\text{A-5})$$

Thus, we have shown that, given that an earthquake has a LASA magnitude $m_L = y$, then the true magnitude m will be normally distributed:

$$E(m/m_L = y) = y - b_L - b\sigma_L^2 \quad (\text{A-6})$$

$$\text{Var}(m/m_L = y) = \sigma_L^2 \quad (\text{A-7})$$

This is a quite interesting result, which says in effect that even if LASA magnitudes m_L were unbiased for any given event (i. e., $b_L = 0$), the expected value of the true magnitude, given the value of m_L , would be different from m_L . At first this may appear to be somewhat surprising, but it can intuitively be explained as resulting from the skew magnitude distribution of earthquakes. As an illustration, consider the following example, assuming $b_L = 0$: Earthquakes of true $m = 4.0$ and $m = 5.0$ have the same probability of being seen at LASA with $m_L = 4.5$. However, since there are many more earthquakes of $m = 4.0$ than of $m = 5.0$, it follows that among all the earthquakes of $m_L = 4.5$; many more will have a true $m = 4.0$ than $m = 5.0$. Therefore, given that $m_L = 4.5$, the probabilities favor $m = 4.0$ over $m = 5.0$ as the value of the true magnitude.

2. Distribution of the NORSAR Magnitude, Given the LASA Magnitude

Closely related to the topic described under 1. is the problem of determining the probability distribution of NORSAR magnitude m_N , given that the LASA magnitude for an event is $m_L = y$.

In order to find this distribution, we first recall that, given m_L , then the true magnitude m has a probability distribution $h(m/m_L)$ defined by (A-5). Furthermore, for each given m , the probability density function $g_N(m_N/m)$ according to our basic assumptions is given as:

$$g_N(m_N/m) = \left(2\pi\sigma_N^2\right)^{-1/2} \cdot e^{-\frac{(m_N - (m + b_N))^2}{2\sigma_N^2}} \quad (\text{A-8})$$

It then follows that the conditional distribution $f(m_N/m_L)$ of m_N given m_L can be expressed as:

$$f(m_N/m_L) = \int_{-\infty}^{\infty} h(m/m_L) \cdot g_N(m_N/m) dm \quad (\text{A-9})$$

After evaluating this integral, we find again a normal distribution, with expectation and variance as follows:

$$E(m_N/m_L) = m_L + (b_N - b_L) - b\sigma_L^2 \quad (\text{A-10})$$

$$\text{Var}(m_N/m_L) = \sigma_L^2 + \sigma_N^2 \quad (\text{A-11})$$

3. An Example of Application

The expressions (A-10) and (A-11) for the conditional expectation and variance of NORSAR magnitude m_N , given LASA magnitude m_L , can easily be illustrated by considering a plot of NORSAR magnitudes versus LASA magnitudes. Figure A-1 presents such a plot for the Kurile Islands aftershock sequence June 17-20, 1973. This example was also addressed in

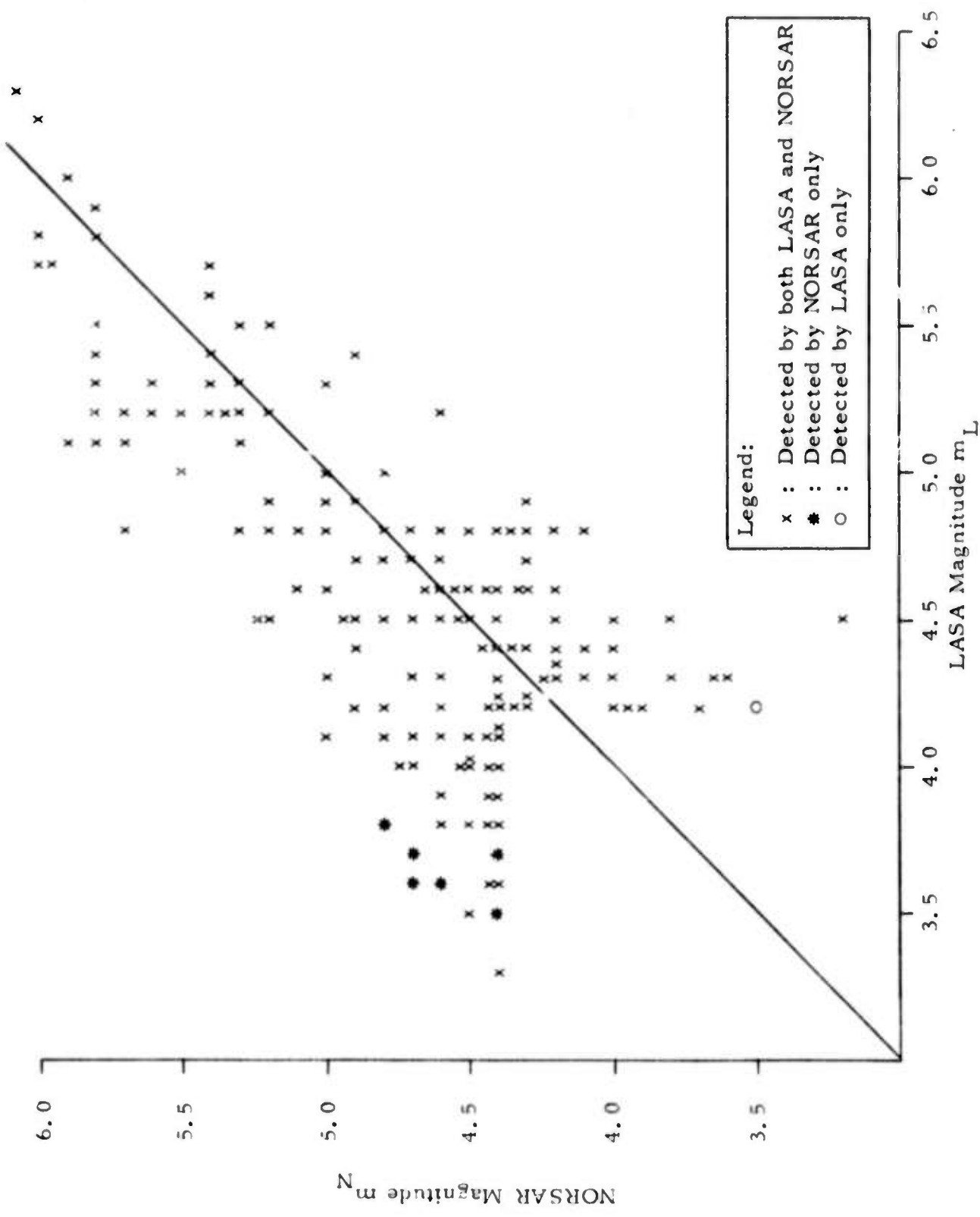


FIGURE A-1
 NORARSAR VERSUS LASA BODYWAVE MAGNITUDES FOR EVENTS FROM THE
 KURILE ISLANDS AFTERSHOCK SEQUENCE JUNE 17-30, 1973

Section IV. All earthquakes with either $m_N \geq 4.4$ or $m_L \geq 4.2$ were included, provided both arrays were operational. For events that were not detected by both arrays, the missing magnitudes were set equal to the apparent 50 percent detection threshold. (It is important not to delete such events, since the resulting diagram then would not reflect the true spread of the magnitude distribution.) The cutoff limits 4.4 and 4.2 were chosen somewhat arbitrarily, with the main consideration being to reduce the number of non-detected events.

According to equation (A-10), the regression curves of Figure A-1 will be parallel, straight lines. We obtain from (A-10) and the symmetric expression of $E(m_L/m_N)$ that:

$$E(m_N - m_L / m_L) + E(m_L - m_N / m_N) = -b(\sigma_N^2 + \sigma_L^2) = -b\sigma^2 \quad (\text{A-12})$$

Similarly, we obtain from (A-11) that

$$\text{St. Dev}(m_N/m_L) = \text{St. Dev}(m_L/m_N) = \sigma \quad (\text{A-13})$$

We recall that, when discussing this same example in Section IV, we obtained estimates of $b' = 0.72$ (base 10) in Figure IV-10, and $\sigma = 0.40$ in Figure IV-8, using equation (IV-2). Therefore the right hand side of (A-13) becomes 0.40, and the right hand side of (A-12) becomes $-2.3 \cdot 0.72 \cdot 0.16 = -0.265$. We can now verify numerically that (A-12) and (A-13) hold true in this particular case by evaluating the left hand side of the two expressions directly from Figure A-1.

Doing this, we obtain the following results, when averaged over all magnitudes:

$$\text{St. Dev}(m_N/m_L) = 0.39 \quad (\text{A-14})$$

$$\text{St. Dev}(m_L/m_N) = 0.38 \quad (\text{A-15})$$

$$E(m_N - m_L/m_L) = 0.01 \quad (\text{A-16})$$

$$E(m_L - m_N/m_N) = -0.30 \quad (\text{A-17})$$

It is seen that (A-14) and (A-15) compare well with the expected result of 0.40, while the sum of (A-16) and (A-17) is -0.29, which also is close to the expected number of -0.265.

Because of lack of data, we cannot use this example to verify that the regression curves actually are straight lines, but we may still conclude that the numerical result found above gives good support to the theoretical model presented earlier.

4. The LASA Seismicity Curve Compared to the True Curve

A natural question to ask at this point is how the distribution of earthquake magnitudes affects the seismicity curve measured at a given seismic station. Specifically, let us assume that the "true" seismicity curve has the form $N(x)$ given by (A-1), and that the LASA curve is

$$N_L(y) = e^{a^* - b^*y} \quad (\text{A-18})$$

where $N_L(y)$ is the number of earthquakes occurring with LASA magnitude exceeding y .

We can find N_L by evaluating the following integral:

$$N_L(y) = \int_y^\infty \left[\int_{-\infty}^\infty N'(x) \cdot g_L(m_L/m=x) dx \right] dm_L \quad (\text{A-19})$$

where g_L is given by (A-4). Informally, the inner integral is the sum over all x of the number of events of true magnitude x times the probability that the LASA magnitude is m_L , given x .

Upon evaluating the integral, we obtain:

$$N_L(y) = e^{a + \frac{1}{2} b^2 \sigma_L^2 - b \cdot (y - b_L)} \quad (\text{A-20})$$

Thus, by comparing (A-18) and (A-20), we have found that

$$a^* = a + b \cdot b_L + \frac{b^2 \sigma_L^2}{2} \quad (\text{A-21})$$

$$b^* = b \quad (\text{A-22})$$

The conclusion is therefore that when estimating seismicity based on only one station, the estimate of b will be unbiased relative to the true value, while this is not usually true for the estimate of a . This assumes, of course, that the estimation method itself does not introduce an additional bias.